Polymer Chemistry

REVIEW

View Article Online
View Journal | View Issue

Cite this: *Polym. Chem.*, 2019, **10**, 1036

Trends in polymeric shape memory hydrogels and hydrogel actuators

Jiaojiao Shang,[a] Xiaoxia Le,[b] Jiawei Zhang,[b] Tao Chen *[b] and Patrick Theato *[c,d]

Received 4th September 2018,
Accepted 11th January 2019

DOI: 10.1039/c8py01286e

rsc.li/polymers

Recently, "smart" hydrogels with either shape memory behavior or reversible actuation have received particular attention and have been further developed into sensors, actuators, or artificial muscles. These three-dimensional polymer networks with the capability of shape deformations show a volume phase transition after being triggered by external physicochemical stimuli. Here, we review the recent advancements and the different types of shape memory hydrogels (SMHs). In addition, stimuli-responsive hydrogel actuators have been investigated with a special focus on their stimulation, their motion-deformation strategies and on the fabrication technologies adopted in hydrogel-based actuators, and finally their applications are described and discussed using specific examples.

1. Introduction

Hydrogels are water-swollen three-dimensional polymeric networks that have been investigated by researchers due to their exceptionally promising potential in a wide range of applications, such as drug delivery,[1–3] sealing,[4–6] tissue engineering,[7–9] actuators,[10–12] *etc.* Compared to the corresponding bulk polymer films, hydrogels with a large amount of water are soft and flexible enough to enable deformations. Additionally, the highly open structure, the large inner surface, and the 3D network of hydrogels are desirable for bioapplications as biosensors and actuators.[13] Particularly, stimuli-responsive behaviors inspired by nature, such as the opening and closing of flowers and the release of seeds from pine cones are affected by light or temperature, and are among the most attractive features of hydrogels that have gained special attention. Generally, hydrogels with "smart" behaviors undergo reversible shape deformations in response to external stimuli, such as heat, light, or electricity. Nowadays, as two of the most famous "smart" hydrogels, shape memory hydrogels (SMHs) and hydrogel actuators (HAs) have attracted increasing attention due to their promising potential applications in biomedicine[14] and soft robotics,[15] and as artificial muscles[16] or as micro-swimmers.[17]

SMHs, as the name implies, are able to fix temporary shapes and recover to their original shape by forming or destructing reversible crosslinks upon external stimuli (*e.g.* by heat, magnetism, light and chemicals). Usually, during this process, some networks of SMHs maintain their permanent shape, and dynamic networks are applied for shape memory.[18,19] Up to now, there have been three main trends in SMH research, such as tough SMHs, triple-/multi-SMHs and multifunctional SMHs.[20,21] Due to the introduction of reversible interactions into hydrogel systems for achieving a shape memory behavior, SMHs tend to have weak mechanical properties. As a result, various approaches, including constructing double networks, dual/triple crosslinks in a single network, have been developed for fabricating tough SMHs. Since the number of temporary shapes can have an effect on promising applications, SMHs with a triple-/multi-shape memory effect have attracted broad attention. What's more, SMHs with a single function can no longer meet the request for wider potential applications. Hence, functions such as self-healing behavior, thermoplasticity, and adhesion properties have already been integrated into SMHs.[22–25] Different from SMHs, without a bonding/bond-breaking process, HAs' actuation performance is due to asymmetric swelling. HAs are based on stimuli-responsive synthetic polymers that are able to swell and shrink in water in response to the changes of environmental stimuli. Since the volume phase transition was first referred to by Tanaka,[26] many hydrogel actuators have been developed as soft actuators due to their flexible and soft characteristics, but also using mimetic motion without the use

[a]*Institute for Technical and Macromolecular Chemistry, University of Hamburg, Bundesstrasse 45, D-20146 Hamburg, Germany*
[b]*Department of Polymers and Composites, Key Laboratory of Bio-based Polymeric Materials Technology and Application of Zhejiang Province, Ningbo Institute of Materials Technology and Engineering, Chinese Academy of Sciences, 1219 Zhongguan West Road, 315201 Ningbo, Zhejiang, China*
[c]*Institute for Chemical Technology and Polymer Chemistry, Karlsruhe Institute of Technology (KIT), Engesser Str. 18, D-76131 Karlsruhe, Germany*
[d]*Institute for Biological Interfaces III, Karlsruhe Institute of Technology (KIT), Herrmann-von-Helmholtz-Platz 1, D-76344 Eggenstein-Leopoldshafen, Germany. E-mail: tao.chen@nimte.ac.cn, patrick.theato@kit.edu*

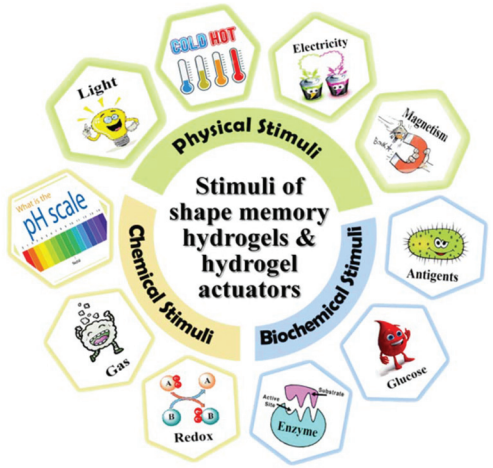

Fig. 1 Schematic illustration of stimuli of shape memory hydrogels and hydrogel actuators.

of mechanical devices, generated from the volume phase transition of crosslinked polymer hydrogels. For HAs, the structures of designed hydrogels determine their response time, application, sensing, actuation and shape changes. Furthermore, the deformation of hydrogels depends mainly on their inhomogeneous structures. Hence, the design principles of hydrogel actuators based on inhomogeneous structures have been described in many reports.[27–29] Nowadays, thanks to the rapid development of microtechnology, technologies for fabricating and designing subtle actuators, which meet the necessity of soft actuators used in microscales, have achieved promising growth. In this aspect, photo-lithography and 3D printing are the most representative techniques adopted in the development of hydrogel-based actuators to prepare hydrogels that mimic behaviors from nature, such as self-folding, twisting and bending in the absence of changes of specific environmental stimuli. Therefore, hydrogel actuators have been used in designing micromanipulators,[30] sensors,[31] optical devices[13] and microfluidic devices.[32]

This review highlights stimuli-responsive hydrogels (stimuli are summarized in Fig. 1), focusing in particularly on shape memory hydrogels (SMHs) and hydrogel actuators (HAs). Main developing trends of SMHs are firstly presented, including toughening SMHs, SMHs with a triple-/multi-shape memory effect and multifunctional SMHs. And then, a brief overview is given of hydrogel actuators with respect to their stimuli, motion-deformations, the technologies and their applications in specific examples.

2. Shape memory hydrogels

2.1 Tough shape memory hydrogels

Because of the weak bonding energy of reversible interactions, SMHs based on only exchangeable bonds usually suffer from poor mechanical properties. However, low strength hydrogels would lose their great potential for use in load-bearing applications. Thus, there is an urgent need to improve the mechanical properties in an appropriate way. Many strategies have been applied to enhance the mechanical properties, including tensile strength, compressive strength and toughness, for contributing to strong hydrogels, which can also be used for SMHs for example constructing particular structures (double network, dual/triple crosslinks in a single network) or doping nanomaterials, *etc.*

It is well known that double network (DN) structures could improve the mechanical properties effectively, in which one network acts as a sacrifice network for energy dissipation and the other serves as an elastic network to keep permanent shapes.[33–37] Similarly, SMHs usually have two different crosslinks, either forming a physical network or chemical network, one of which is for fixing temporary shapes and one for maintaining original shapes. Thus, the reversible switches used for the shape memory effect can also play an important part in strengthening the toughness of hydrogels. For example, Weiss *et al.* prepared a tough hybrid hydrogel having both physical and covalent cross-links, and it can achieve shape memory behavior through the switching of glassy nanodomains at a certain temperature.[38] By integrating a physically cross-linked gelatin network and a chemically cross-linked PAAm network with graphene oxide (GO), Tong's group realized NIR-triggered shape memory performance, in which both the gelatin network and the GO bridging take part in dissipating deformation energy.[39]

According to a similar mechanism of energy dissipation, the construction of dual/triple crosslinks in a single network is another effective approach to render SMHs with good mechanical properties. For instance, in the system designed by Wang *et al.*, strong multiple hydrogen bonds form between poly(vinyl alcohol) (PVA) and tannic acid (TA) molecules, functioning as permanent crosslinks, while weaker hydrogen bonds between PVA chains act as reversible interactions for shape memory and shape recovery. The breaking and the formation of the weaker hydrogen bonds also play the role of sacrificial bonds to endow hydrogels with excellent mechanical properties (Fig. 2).[40]

2.2 Triple-/multi-shape memory hydrogels

Previous SMHs, possessing a dual shape memory effect, can only remember one simple temporary shape in each shape memory cycle. Since the number of temporary shapes that can be fixed will affect the potential applications of SMHs, more and more attention has been paid to the fabrication of triple-/multi-shape memory hydrogels. Nowadays, there are three main ways to endow SMHs with triple-/multi-shape memory effects, which are summarized in the following.

2.2.1 Single stimulus-induced triple-shape memory effect. Responses of SMHs to a single stimulus may be realized when different temporary crosslinks feature varying levels of sensitivity to one stimulus, resulting in triple-/multi-shape memory performance. An early representative example is presented by Liu's group, in which the first SMH with a triple shape memory effect was explored (Fig. 3-I). The association and dissociation of both dipole–dipole interactions between nitrile

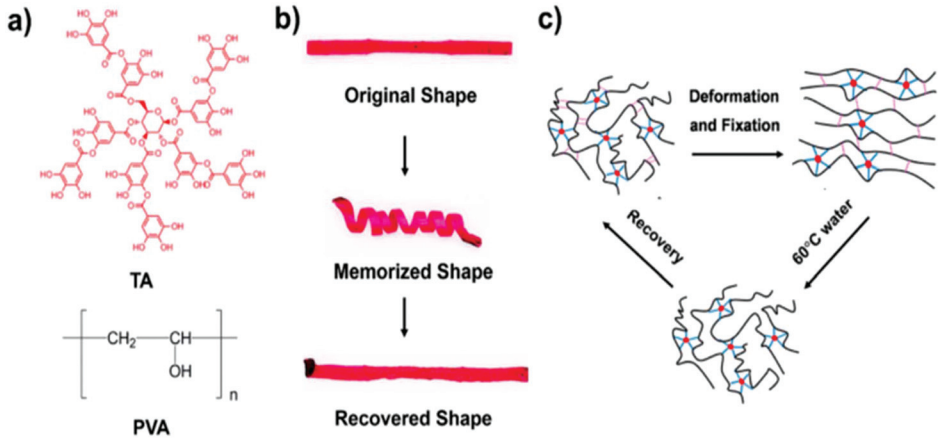

Fig. 2 PVA–TA SMHs with excellent mechanical properties (reproduced from ref. 40 with permission of the American Chemical Society).

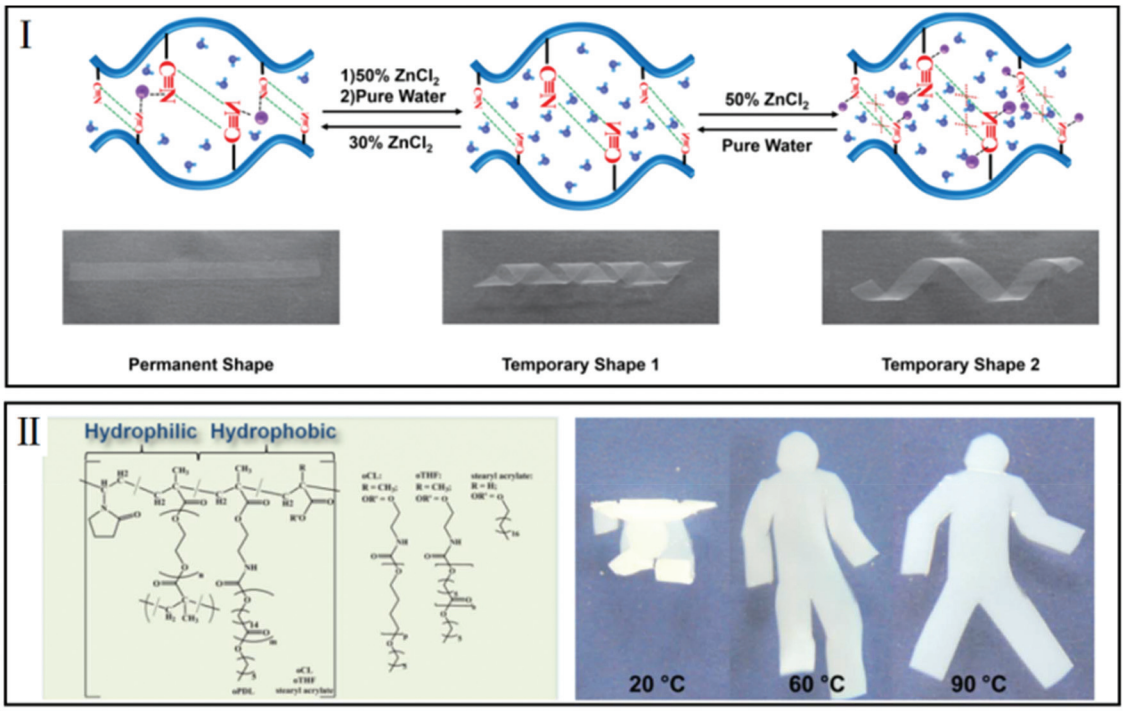

Fig. 3 Single-stimuli-induced triple-shape memory effect. (I) Zn^{2+} triggered triple memory effect by managing the interactions of CN–CN and Zn–CN (reproduced from ref. 41 with permission of John Wiley and Sons); (II) heat-triggered triple shape memory effect at different temperatures because of two types of semicrystalline side chains (reproduced from ref. 42 with permission of the American Chemical Society).

groups (CN–CN) and Zn–CN linkage can be adjusted by the concentration of zinc ions, leading to a triple shape memory behavior.[41]

As one of the most commonly used stimuli, heat can be employed to design SMHs with a triple-/multi-shape memory effect due to the different forces generated from different interactions. Hydrogels reported by Lendlein *et al.* are composed of two different types of hydrophobic crystallizable switching segments, corresponding to two different switching temperatures (Fig. 3-II). During the programming procedure of changing the temperature, two distinct temporary shapes can be memorized and recovered through crystallization and amorphization of hydrophobic side chains.[42]

2.2.2 Different stimuli-triggered triple-/multi-shape memory effects. As different stimuli can be introduced step by step, combining non-interfering interactions in one material provides an efficient way to create triple-/multi-shape memory materials. Typical examples are the stretchable supramolecular hydrogels with a triple-shape memory effect such as those fabricated by Chen's group (Fig. 4-I). By sequentially introducing two independent interactions, including alginate–Ca^{2+} chelation and phenylboronic acid (PBA)–diol ester bonds, into a

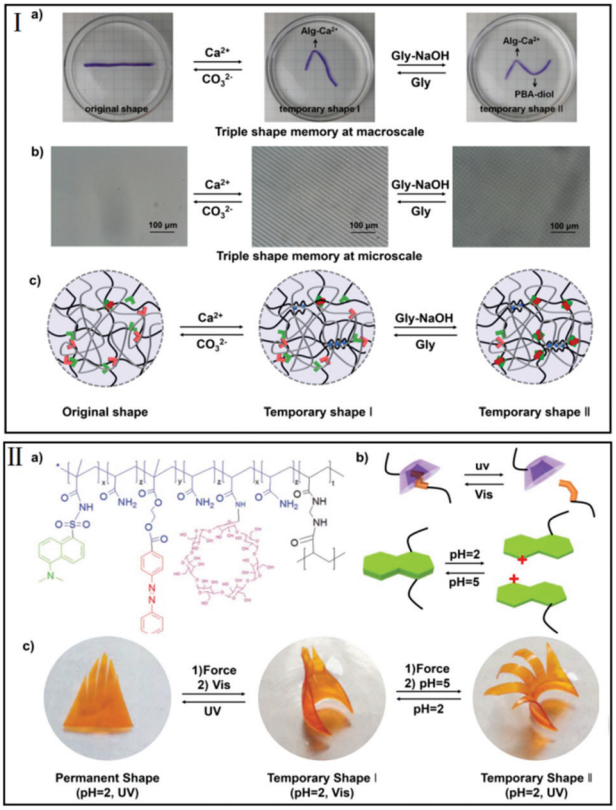

Fig. 4 Different stimuli-triggered triple-shape memory effects. (I) Triple-shape memory effects at both the macroscale and microscale have been achieved by programmable introduction of Alg–Ca^{2+} chelation and PBA–diol ester bonds (reproduced from ref. 43 with permission of the Royal Society of Chemistry); (II) triple-shape memory effect realized by adjusting pH and UV/Vis stimuli (reproduced from ref. 46 with permission of the American Chemical Society).

double-network system, an impressive triple-shape memory performance has been successfully achieved at both the macro-scale and micro-scale.[43] In addition, utilizing one interaction for the shape memory effect and another interaction for self-healing, shape memory behavior after the self-healing process or self-healing procedure during shape memory performance can also be realized. Similarly, Schiff base bonds and metal coordination interactions can also be integrated for realizing the triple shape memory properties.[44] The reversible Schiff base bonds between the amino groups of chitosan and aldehyde groups of oxidized dextran could be applied to memorize temporary shapes. Meanwhile, various metal cations can also chelate with chitosan for fixing other temporary shapes. Furthermore, in order to obtain a multi-shape memory effect, Chen's group combined three different forces programmably, including PBA–diol ester bonds, AAc–Fe^{3+} and coil–helix transition of agar.[45] Besides the multi-shape memory effect, the obtained new shape memory hydrogel featured tunable mechanical properties through simply changing soaking time in the corresponding solutions.

As shown in Fig. 4-II, a light-, pH-, and thermo-responsive hydrogel with a triple-shape memory effect was prepared by introducing dansyl-aggregations and host–guest interactions on the basis of azobenzene (Azo) with cyclodextrin (β-CD). Since the aggregation of dansyl groups at a high pH value and the supramolecular inclusion complexes of β-CD-Azo under visible light can act as reversible switches, a triple-shape memory effect can be realized in response to light and pH sequentially.[46] And, what is more, the reversible aggregation–disaggregation transition of the dansyl group can respond to both pH and temperature, thus the hydrogels showed a triple-shape memory behavior by controlling the programming process.[47]

2.2.3 Time-controlled multi-shape memory effects. Another simple method to realize a multi-shape memory effect is by adjusting the processing time. By altering the time for memorizing shapes, different temporary shapes can be fixed. As an example for a time-controlled multi-shape memory, a PAA–Go–Fe^{3+} hydrogel with a dual physically cross-linked structure was synthesized (Fig. 5-I).[48] By adjusting the immersing time in $FeCl_3$/HCl and pure water, four different temporary shapes were fixed because of the formation types between Fe^{3+} and acrylic acid (AAc) (mono-, bi-, and tridentate). Furthermore, by changing the soaking time in HCl, the shape-memorized hydrogel recovered sequentially to its original shape. Another typical example was presented by Chen's group.[49] Reversible physical interactions, including chitosan microcrystals and chain-entanglement crosslinks, can be achieved simply by soaking chitosan in NaOH and NaCl solutions, respectively. Due to the diffusion transition mechanism, the stimulating chemical (NaOH solution or NaCl solution) diffuses from outside of the hydrogel to the inside for fixing temporary shapes step by step, implementing a multi-shape memory effect (Fig. 5-II).

2.3 Multifunctional shape memory hydrogels

Since a single function can often not meet all requirements for practical applications, it is quite promising to develop SMHs with multi-functionalities, such as self-healing, self-adhesion, thermoplasticity as well as antibacterial and anti-inflammatory functions.

2.3.1 SMHs with self-healing behavior. Since the service life of materials is an important index for materials, self-healing materials can restore their functionalities after damage, which is also of great significance for SMHs. Experts have done a considerable amount of research to endow SMHs with a self-healing performance. Chen *et al.* first constructed a supramolecular hydrogel with both self-healing and shape memory properties,[50] which was based on dynamic PBA–diol ester bonds and the formation of an alginate–Ca^{2+} complex, respectively. Li *et al.* prepared a double network hydrogel composed of a poly(ethylene glycol) (PEG) network and a poly(vinyl alcohol) (PVA) network.[51] The former chemically cross-linked network was used to maintain the permanent shape, and the latter one, which was physically cross-linked, can be applied for both shape memory and self-healing (Fig. 6-I), as the two bonding motifs do not interfere with each other.

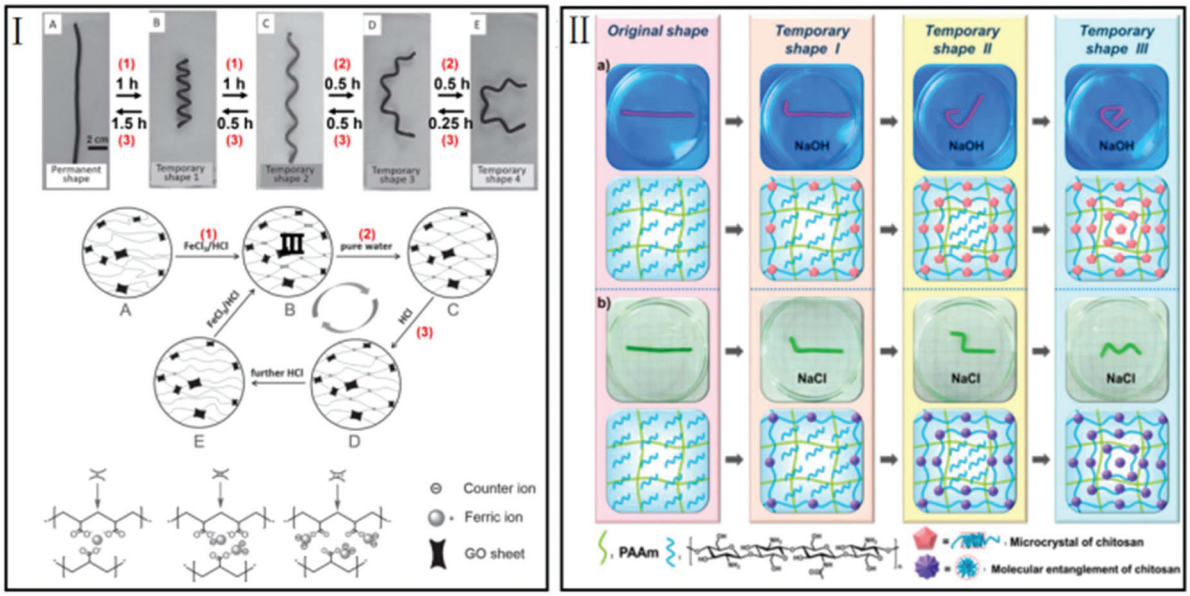

Fig. 5 Time-controlled multi-shape memory effect. (I) Adjusting the types of formation between Fe^{3+} and AAc (mono-, bi-, and tridentate) by changing the immersing time in a $FeCl_3$/HCl or HCl solution for multi-shape memory (reproduced from ref. 48 with permission of John Wiley and Sons); (II) different degrees of formation of microcrystals or molecular entanglement of chitosan for multi-shape memory (reproduced from ref. 49 with permission of MDPI).

2.3.2 SMHs with thermoplasticity. Among all the functions, thermoplasticity is a particularly attractive one. Once thermoplasticity is introduced into SMHs, the permanent shape can be changed, which means SMHs can possess various permanent shapes, leading to more temporary shapes. A hydrophobic polyampholyte SMH reported by Yang *et al.* possesses a unique thermoplasticity, which can change its permanent shape upon heating.[52] Through either ligand–ion bindings or salt-dependent hydrophobic association, temporary shapes can be memorized. Recently, a novel dual cross-linked single-network hydrogel has been fabricated through copolymerization of acrylamide (AAm) and AAc with *n*-octadecyl acrylate.[53] Without any chemical cross-linkers, the hydrogel exhibited an intriguing thermoplasticity. In addition, an alternative use of vitamin C (Vc) and Fe^{3+} induced the shape memory and the shape recovery process (Fig. 6-II).

2.3.3 SMHs with actuating behavior. Up to now, the temporary shapes of presently existing SMHs are usually created by manual deformation. However, this simple method will be limited when it comes to the preparation of complex temporary shapes, which is difficult to manipulate by hands. Inspired by the design thinking of hydrogel actuators, SMHs with actuating behavior have been reported. For example, a bilayer shape memory hydrogel has been fabricated within a thermo-responsive actuating layer and a pH-responsive memorizing layer.[54] In the system, one layer made of PNIPAM hydrogel shrank at higher temperature, leading to the self-deformation of the whole hydrogel. After that, the other layer containing chitosan could form micro-crystals for stabilizing temporary shapes when soaking in base solution. By using photo-masks, more complex temporary shapes could be achieved due to local deformation.

In addition, another anisotropic hydrogel with integrated self-deformation and controllable shape memory effect has also been reported by Chen's group. Through constructing an anisotropic PAAc–PAAm structure, the obtained hydrogel deformed into certain shapes in response to pH stimulus, which can be fixed by the coordination between carboxylic groups and Fe^{3+}. Moreover, the shape memory ratio and shape recovery ratio could be adjusted with the concentration of the corresponding ions, such as Fe^{3+} and H^+.[40]

2.3.4 SMHs with other functions. In order to adapt to complex situations, SMHs are now designed to have more and more functions. A novel supramolecular hydrogel possessing a self-healing function, a shape memory and an adhesion property has been reported.[55] Since Ca^{2+} can chelate with alginate for keeping permanent shapes, the association and dissociation of dynamic phenylboronic acid (PBA)–catechol interactions could be applied for a shape memory and self-healing performance. In addition, the catechol moieties endow the hydrogel with perfect adhesive properties. Besides shape memory, antibacterial and anti-inflammatory functions have been integrated to fabricate multi-walled hydrogel tubes for a potential tissue engineering scaffold.[56]

3. Stimuli-responsive hydrogel actuators

3.1 Design principles and strategies for fabricating a hydrogel-based actuator

The main principle of movement in nature tissue is based on the discrepant part in nonuniform swelling. In order to create

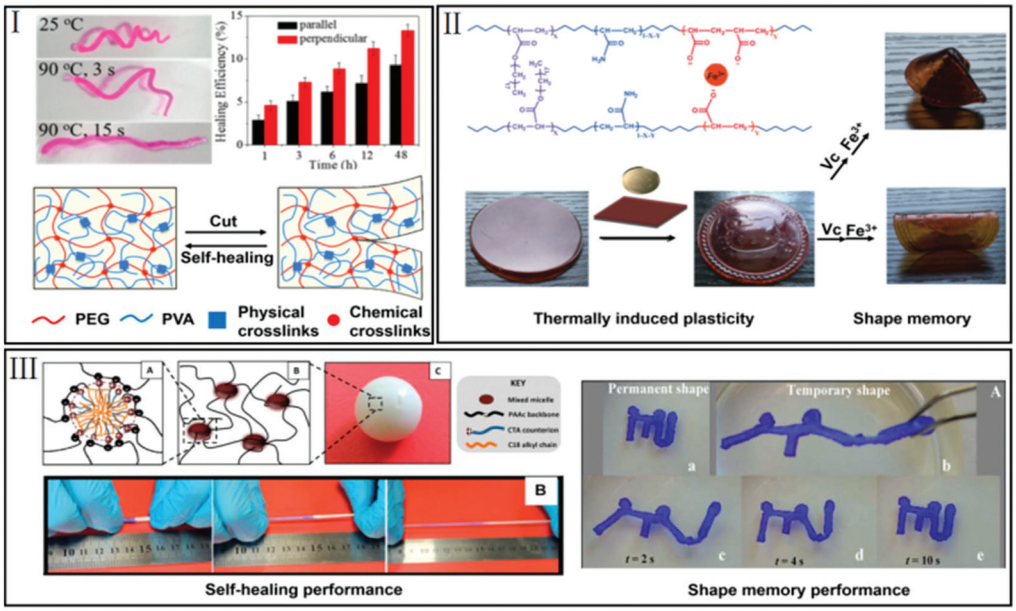

Fig. 6 SMHs with other functionalities. (I) SMHs with self-healing behavior (reproduced from ref. 51 with permission of the American Chemical Society); (II) SMHs with thermoplasticity (reproduced from ref. 52 with permission of the Royal Society of Chemistry); (III) SMHs with self-healing and high mechanical strength (reproduced from ref. 53 with permission of the American Chemical Society).

a self-folding deformation, a generated bending in a hydrogel sheet resulting from differential stress either along its thickness or its lateral dimensions is necessary.[57] Up to now, several strategies have been developed to fabricate smart hydrogels with inhomogeneous structures. One approach is to fabricate discrepant distributions in the structure of responsive hydrogels (Fig. 7), such as (i) a hydrogel with inhomogeneous cross-linked dots, which generates deformation when asymmetrical swelling occurs due to highly crosslinked dots within a low crosslinked matrix allowing cross-linking to be adjusted by irradiation dose[58] (Fig. 7-I), (ii) "bistrip" hydrogels with variations in the degree of crosslinking and hence possessing varying degrees of swelling making the hydrogel to shrink, unroll and recover a flat shape when the temperature of the aqueous medium changes[59] (Fig. 7-II), (iii) imprinting Cu^{2+} ion complexes locally with anionic hydrogels to fabricate stiffer ionoprinted regions, which guide the asymmetric shrinking and reshaping of the gel structure[60] (Fig. 7-III), or (iv) heterogeneous porous structures by using a one-step evaporation process to create a laminated layer/porous layer heterogeneous structure in a vertical direction and pattern the heterogeneous structure in a lateral direction to form tunable, fast, and robust hydrogel actuators[61] (Fig. 7-IV). Typically, variation in irradiation time endows the hydrogel regions with different crosslinking densities and hence the resulting hydrogel areas show different swelling/deswelling properties, which further result in the generation of in-plane stress. As a result, shape deformations occur in the hydrogel matrix. This means that the shape deformation of the hydrogels can be programmed, *e.g.*, by using variations of photolithographic patterns to generate areas with different crosslinking degrees or to change the structure of surface features to yield asymmetric shrinking and reshaping.[62,63] Another straightforward strategy is to create a bilayer hydrogel with discrepant swelling layers in the longitudinal axis, which generates bending stress due to the differences in swelling degrees.[64–67]

Here, some examples of bilayer hydrogels used for actuators are listed. Noy Bassik *et al.*[64] fabricated hydrogel bilayers, derived from *N*-isopropyl-acrylamide (NIPAM), acrylic acid (AA), and poly(ethylene oxide)diacrylate (PEODA), which can fold and unfold in response to changing aqueous solutions having different pH values and ionic strengths (Fig. 8-I). These actuators are composed of two layers with different swelling behaviors and were prepared by combining spin coating and photolithographic patterning techniques. Of these two layers, the pH-responsive layer swells in solution with a pH above the pK_a of the hydrogel due to the ionization and subsequent dissociation of the acid group in the hydrogel, whereas the passive layer has no response. As a result, an osmotic pressure generated between the surface and inside the hydrogel causes the folding behavior due to the difference in mobile ion concentration as governed by the Donnan equilibrium. Zhao *et al.*[65] prepared bilayer- and multilayer-hydrogel actuators using a PAA gel reinforced by further cross-linking with Fe^{3+} ions (Fig. 8-II). These hydrogel actuators showed a rapid response and a precise control of the direction of action in the media having different pH values and ionic strengths. Li *et al.*[66] fabricated temperature- and pH-responsive semi-interpenetrating network (semi-IPN) hydrogel-based bilayer actuators by generating a PNIPAM based hydrogel in the presence of PDADMAC on a layer of gold-coated polydimethylsiloxane (PDMS) (Fig. 8-III). These bilayers exhibit a revisable and

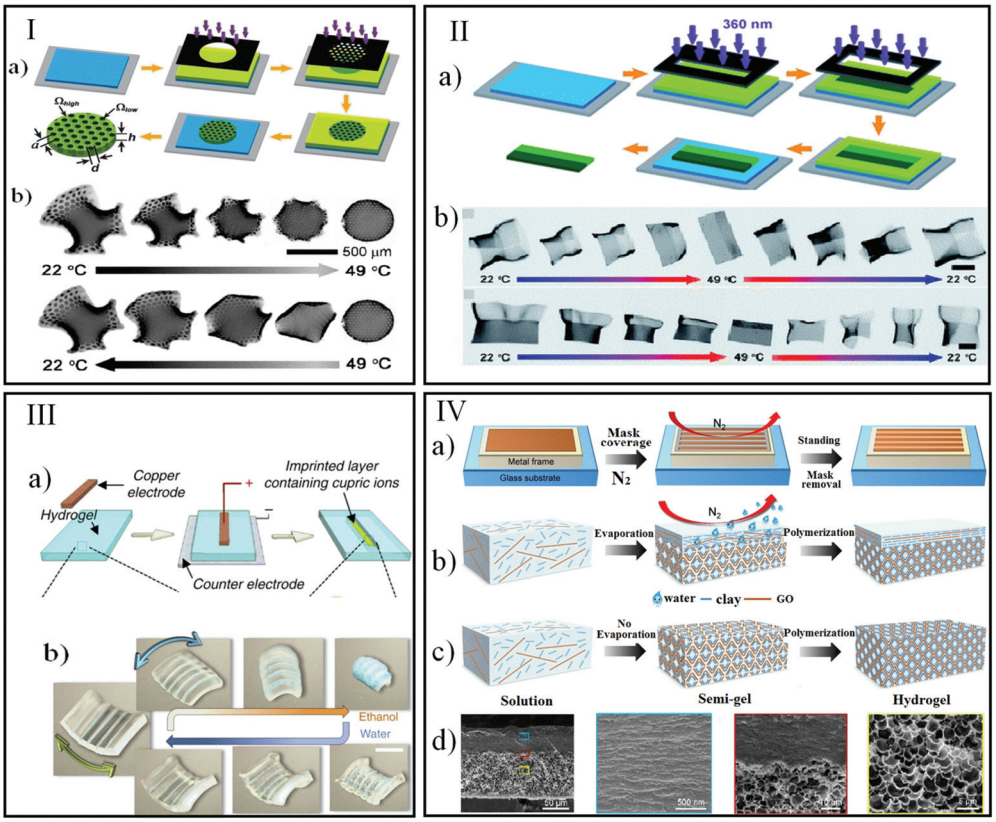

Fig. 7 Fabrication and swelling-induced deformation of inhomogeneous hydrogels: (I) highly crosslinked dots within a low crosslinked halftone gel matrix. Reproduced with permission from ref. 58. Copyright 2012, American Association for the Advancement of Science; (II) hydrogel with variations in the degree of crosslinking. Reproduced with permission from ref. 59. Copyright 2012, Royal Society of Chemistry; (III) patterned stiffer ionoprinted regions on anionic hydrogels causing asymmetric shrinking and reshaping of the gel structure in EtOH (ethanol) and water. Reproduced with permission from ref. 60. Copyright 2013, Nature Communications; (IV) heterogeneous porous structures by using a one-step evaporation process to create a laminated layer/porous layer heterogeneous structure in a vertical direction. Reproduced with permission from ref. 61. Copyright 2017, American Chemical Society.

repeatable thermoresponsive and pH-responsive bending and unbending behavior and can be used as soft grippers.

3.2 Stimulation of "smart" hydrogels

"Smart" hydrogels with controllable volume/shape changes in response to external physical or chemical/biochemical stimuli have become promising stars in developing mimetic actuators for controllably triggered manipulation.[68–73] In general, physical stimuli, including temperature,[74] electrical signals,[75] magnetic fields,[17] or mechanical stress,[76] alter molecular interactions at critical onset points. However, chemical stimuli, such as pH,[77] ionic factors,[78] and chemical agents, will change the interactions between polymer chains or between polymer chains and solvent at the molecular level. Recently, biochemical stimuli have been considered as another category and involves responses to antigens,[79] enzymes,[80] ligands,[81] and other biochemical agents.[82–84] In order to explore and mimic the more complex stimulation systems from nature, more researchers have developed novel hydrogel systems in which two or more stimuli-responsive mechanisms are combined, the so-called dual-responsive and multi-responsive hydrogel systems.[85–88]

3.2.1 Physical stimuli. By far the most studied and best understood response is that to temperature, which is one of the most favorable environmental stimuli that is used to trigger hydrogel systems that undergo sol–gel phase transitions or volume change at a critical solution temperature.[89–93] Temperature-responsive hydrogels that are composed of these materials possess a lower critical solution temperature or an upper critical solution temperature (UCST). Thus, poly(*N*-isopropyl acrylamide) (PNIPAM) as the most well-known example used in thermo-sensitive polymer gels with a lower critical solution temperature (LCST, 32 °C) has been actively studied for application in smart materials.[94–99] PNIPAM hydrogels can swell at temperatures below LCST and shrink upon heating to a temperature above LCST.[100–102] In contrast, hydrogels derived from polymers featuring a UCST show their phase transition at an upper critical solution temperature, which means they can shrink when cooled below their UCST. Examples for such hydrogels are: poly(vinyl methyl ether) (PVME) and poly(ethylene oxide) (PEO). Lee *et al.*[103] fabricated

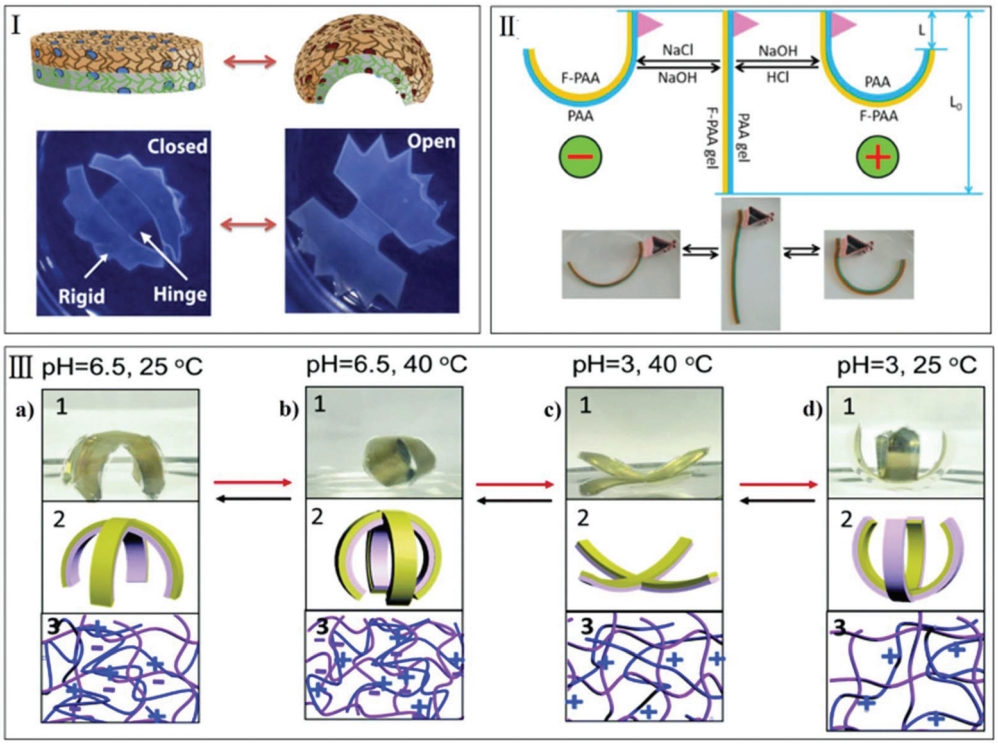

Fig. 8 Bilayer hydrogel actuators. (I) Actuator with hinges folding in changing pH/IS. A VF-shaped actuator constructed from rigid SU-8 segments with a NIPAm–AAc/PEODA bilayer hinge (reproduced from ref. 64 with permission. Copyright 2010, Elsevier Ltd); (II) reversible actuation of the Janus bilayer hydrogel in different solutions (reprinted with permission from ref. 65. Copyright 2017, American Chemical Society); (III) a temperature- and pH-responsive semi-interpenetrating network (semi-IPN) hydrogel-based bilayer actuator (reprinted with permission from ref. 66. Copyright 2017, Royal Society of Chemistry).

a temperature-responsive hydrogel bilayer using an interpenetrating polymer network (IPN) of (PNIPAAm) and PVA. Interestingly, the bending diameter and bending direction of such a bilayer can be controlled by the crosslinking degree of IPN and PVA films. A starfish-shaped gripper showed its temperature-sensitivity by lifting and releasing an object in 25 °C and 37 °C water (Fig. 9-I).

Using an electrical signal as an environmental stimulus to induce responses in hydrogels has received particular attention due to the reliable control of signal strength and direction, remote operation and a precise "on/off" triggering switch. Typical hydrogels that are sensitive to an electrical signal are polyelectrolyte networks, such as polysaccharide and poly(2-acrylamido-2-methylpropanesulfonic acid) (PAMPS). Under electric fields, osmotic pressure gradients are produced due to the asymmetrical distribution of mobile ions in polyelectrolyte networks (electrolyte solution), which induce the shrinking or swelling of the polyelectrolyte hydrogel. In 1965, Hamlen *et al.*[104] observed the expansion and contraction of a poly(vinyl alcohol-*co*-acrylic acid) polyelectrolyte gel induced by an electric field. Since then, an increasing number of electrically-controlled artificial muscles, robots and other smart devices were fabricated using polyelectrolyte polymers based on the electro-induced volume/shape changes.[105–107] For example, Yang *et al.*[105] developed soft hydrogel walkers consisting of polyanionic poly(2-acrylamide-2-methylpropanesulfonic acid-*co*-acrylamide) (P(AMPS-*co*-AAm)) exhibiting an arc looper-like shape with two "legs" for walking in an electrolyte solution. Morales *et al.*[106] fabricated gel actuators with two legs composed of gels that can walk unidirectionally in diluted salt solutions without the need for ratchet surfaces to the electric field (Fig. 9-II).

Light as another promising stimulus was investigated in photo-driven hydrogel actuators benefiting from their numerous advantages such as fast response, remote operation, easy to downsize, controllable intensity, no necessary physical contact with the materials and high efficiency. Photo-responsive hydrogels can be classified into UV-sensitive and visible-light-sensitive hydrogels. Irradiation from a unique light source, the changes in polarity, free volume, and hydrophilicity/hydrophobicity of photo-responsive hydrogel actuators endow them with the corresponding possibility of motion. As reported, typical photo-driven hydrogels were synthesized by introducing photo-sensitive chromophores, such as azobenzene (due to their *cis–trans* photo-isomerization)[108] or spiropyran (ring opening and closing photo-isomerization)[109,110] into the side or main chains of polymers. Additionally, photothermal conversion materials dispersed in thermally responsive hydrogel matrices have been demonstrated to be sufficient for transferring the energy from visible or near-infrared light

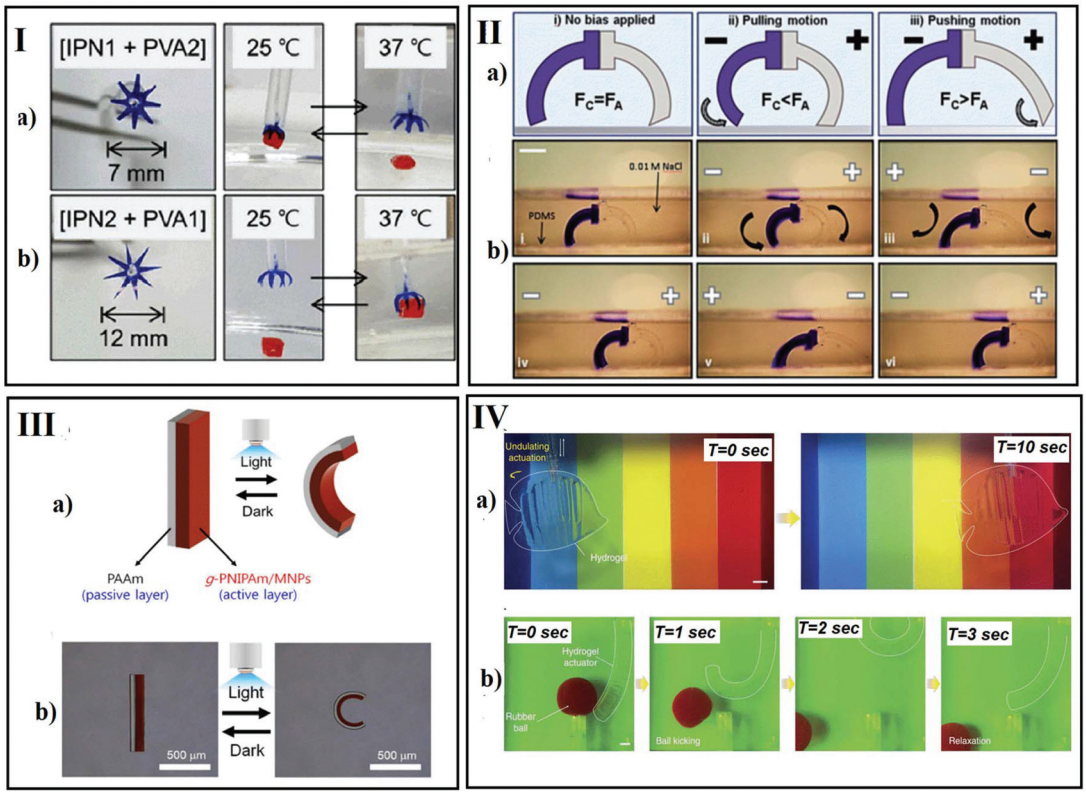

Fig. 9 Hydrogel actuators induced by physical stimuli. (I) Temperature-responsive starfish-shaped gripper. Reprinted with permission from ref. 103. Copyright 2018, Polymer Society of Korea and Springer; (II) light-responsive bidirectional and circular bending actuator. Reprinted with permission from ref. 105. Copyright 2016, Nature publication; (III) hydrogel walker moving in the direction of the applied electric field. Reprinted with permission from ref. 114. Copyright 2014, Royal Society of Chemistry; (IV) hydraulic hydrogel actuators. Reprinted with permission from ref. 121. Copyright 2017, Nature publication.

to thermal energy, further resulting in a volume phase transition of hydrogels. In this case, the main trigger is thermal heat generation by absorption of light in the hydrogel matrix, which triggers volume shrinkage of the temperature-responsive hydrogel. Most research on these photo-thermal materials focuses on carbon-based materials, such as graphene oxide (GO)[111] and metallic nanoparticles such as iron oxide[112] or gold.[113] For example, Lee *et al.*[114] fabricated a fast responding photo-actuator by combining a comb-type PNIPAM hydrogel matrix with magnetite nanoparticles (Fig. 9-III).

Similar to light and an electrical signal, an external magnetic field can also be used to remotely control a magnetically-active hydrogel rapidly. Typically, a magnetically-active hydrogel consists of composites of hydrogel networks filled with magnetic nanoparticles, resulting in direct coupling between the magnetic and the mechanical properties of the magnetically-active polymeric gel, such as distributed metal particles, iron(III) oxide particles[115] or ferromagnetic particles[116,117] attached to the flexible polymer network *via* hydrogen bonding, van-der-Waals forces or, coordination bonds. The rapid and controllable shape changes of these gels would be expected to mimic muscular contraction. Combined with biodegradable and biocompatible polymers, such as poly(D,L-lactide), poly(ε-caprolactone), poly(ethylene glycol) and their copolymer and grafting polymers, these magnetically-active hydrogels have originally been proposed for biomedical applications.[118–120]

Besides the above-mentioned stimuli, pressure is also of interest as an induced trigger for smart hydrogels. Thus, for example, Yuk *et al.*[121] have, inspired by leptocephali, developed hydraulic hydrogel actuators, which can imitate the camouflage capabilities optically and sonically. These hydrogel actuators are also able to kick a ball and catch a live fish owing to the anti-fatigue properties of the hydrogel under moderate stresses (Fig. 9-IV).

3.2.2 Chemical stimuli. In a living system, the concentrations of pH and ions have proved to be particularly important characteristics. As a result, variations of hydrogels made of polymeric backbones with pH-responsive functional groups, such as carboxyl and pyridine, which can accept or donate protons in response to an environmental pH change, were developed for a wide application in drug delivery.[122–124] Based on the principle that the reversible ionization of ionic pendant groups occurred under physiological pH changes, a large osmotic swelling force was created during the volume transition by generating electrostatic repulsive forces between ionized groups. For example, at a low pH, carboxylic pendant groups in poly(acrylic acid) (PAAc) and poly(methacrylic acid)

(PMAAc) hydrogels accept protons, while releasing them at a high pH. The phase transition of polyelectrolytes at a high pH with electrostatic repulsion forces between the molecular chains in combination with hydrophobic interaction causes the deswelling/swelling of hydrogels. As shown in Fig. 10-I, Zhao *et al.*[65] have designed hydrogel actuators with crosslinked PAA-clay triggered by changes in pH or ionic strength. By adjusting the ionic strength or the pH of the medium solution, the swelling ratio and the bending direction of the bilayer actuator could be controlled.

Changing the composition of the solvent in hydrogels, such as a hydrophilic or a hydrophobic chemical solvent, also induced bending and twisting behavior of the hydrogel. For instance, Jeong *et al.*[125] fabricated reversible and color-tunable photonic actuators responding to both hydrophilic and hydrophobic chemical environments (acetic acid and hexane) through a symmetry breaking process and a change in the lattice constant of the photonic crystal structure. In Fig. 10-II, the 2D programmed structure transformed to a 3D cubic object in hexane.

Redox-responsive hydrogels have always been regarded as one of the most promising biomaterial composites for biomedical applications, and have frequently been employed in areas, such as tissue engineering and drug delivery.[126,127] Particularly poly(amido amine)-based redox-responsive hydrogels have, due to their property of being biocompatible and highly versatile, gained significant attention. Greene *et al.*[128] introduced a redox-responsive mechanism of actuation in hydrogels by describing a systematic investigation into the radical-based self-assembly of a series of unimolecular viologen-based oligomeric links. Moreover, an artificial molecular muscle at work was demonstrated (Fig. 10-III).

3.2.3 Biochemical stimuli. Biochemical stimuli, such as glucose, are highly desirable for developing an artificial closed-loop system that is capable of inducing an insulin release in response to a glucose concentration under physiological conditions. Hence, glucose-sensitive hydrogels have received considerable attention because of their potential application in both glucose-sensing and insulin delivery application for treating diabetes mellitus. Typically, glucose-responsive polymeric systems are based on three modes: (i) enzymatic oxidation of glucose by glucose oxidase, (ii) binding of glucose with concanavalin A, and (iii) reversible covalent bond formation between glucose and boronic acids. As far as glucose-

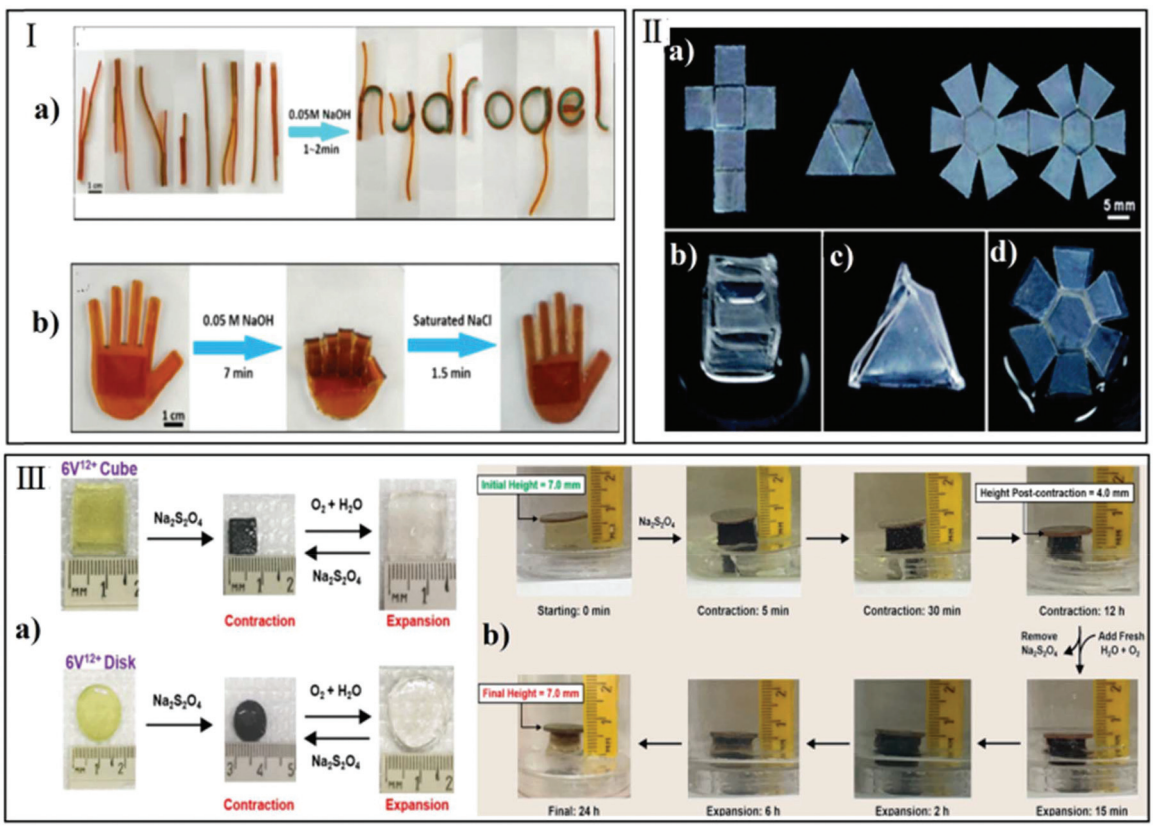

Fig. 10 Hydrogel actuators induced by chemical stimuli. (I) Gel strips assembled by a pH-responsive hydrogel actuator to represent the word hydrogel and the grasp-open action of the hand-shaped actuator. Reprinted with permission from ref. 65. Copyright 2017, American Chemical Society; (II) hexane-responsive hydrogels folded themselves from (a) programmed 2D structures to transformed 3D objects in hexane solvent: (b) cube, (c) pyramid, and (d) phlat ball. Reprinted with permission from ref. 125. Copyright 2011, Royal Society of Chemistry; (III) demonstration of an artificial molecular muscle at work in versene solution and H_2O. Reprinted with permission from ref. 128. Copyright 2017, American Chemical Society.

responsive hydrogels based on glucose oxidase are concerned, the byproducts (gluconic acid and H_2O_2) from enzymatic oxidation of glucose led to glucose responsivity. For example, Imanishi *et al.*[129] reported the covalent modification of a cellulose film with glucose oxidase-conjugated poly(acrylic acid) (PAA). The same applies to pH-responsive behavior, at neutral and high pH levels, and the carboxylate units of the PAA chains were negatively charged and extended due to electrostatic repulsion, which resulted in occlusion of the pores in the cellulose membrane. Conversely, the protonation of the PAA carboxylate units at low pH after the addition of glucose, and the concomitant collapse of the chains closes the membrane pores, with the latter event facilitating the release of entrapped insulin. Since Shiino and Kataoka *et al.*[130] published the first work about utilizing phenyl boronic acid (PBA) as a glucose sensor in hydrogel systems, glucose-responsive hydrogels based on PBA have received increasing attention, owing to their ability to bind with 1,2-diols or 1,3-diols *via* dynamic covalent bonds.[131–140] For example, Meng *et al.*[77] constructed a novel pH- and sugar-induced shape memory hydrogel based on dynamic PBA–diol interactions formed by PBA-modified sodium alginate (Alg-PBA) and poly(vinyl alcohol) (PVA).

Besides the biochemical stimuli mentioned above, antigen enzyme-triggered hydrogels used in biomedical areas have been substantially further developed.[141–143] For example, Athas *et al.*[141] designed "hybrid" hydrogels with a Venus flytrap shape, derived from three individual gels with distinct properties, which can transform from an open to a closed state upon exposure to enzyme, *i.e.*, collagenase or lysate of murine fibroblast cells.

3.2.4 Dual/multi-stimuli used for hydrogel actuators. Because a single stimulus applied for driving a mimic actuator cannot satisfy the complex mechanism of natural living systems, plenty of hydrogel actuators are based on dual/multi-stimuli. Hence, multi-simulative hydrogel actuators would be more intriguing to develop smart devices and have been considered as the most exciting ones. As reported in the literature, systems responding to a combination of two or more signals, such as pH/temperature, pH/ionic strength, temperature/magnetic field, temperature/light, pH/ionic strength/temperature, and temperature/pH/magnetic field have recently been developed.[144–149] For instance, the group of Theato fabricated PNIPAm/PAA composite hydrogels and bilayer hydrogels with a defined lateral and vertical inhomogeneous structure.[149] These hydrogels feature complex 3D deformations upon variation of temperature, ionic strength and pH. Moreover, bilayer hydrogels that feature a self-folding behavior upon stimulation can work as temperature-controlled actuators to achieve the transportation and direction-controllable manipulation of small objects.

3.3 Fabrication technologies adopted in the development of hydrogel-based actuators

Depending on the application and design shape of hydrogel actuators, their dimensions range from nanometers to centimeters. As a result, different fabrication technologies, such as molding, micromolding, dip-coating, lithography, 3D printing, ionoprinting, capillary origami and ion inkjet printing, were utilized in the development of hydrogel-based actuators and are summarized in the following.[150]

3.3.1 Molding. Molding is the most common and simple method to pattern large scale hydrogel actuators with the dimensions ranging from centimeters to millimeters. However, this method needs to be combined with other technologies to prepare a specific mold for each geometrical shape. For example, Duan *et al.*[151] fabricated a hydrogel used for bioinspired lenses, which can carry out rapid, reversible, and repeated self-rolling deformation actuated by pH-triggered swelling/deswelling. Moreover, these hydrogels can transform into rings, tubules, and flower-, helix-, bamboo-, and wave-like shapes by effectively designing the geometric shape and size *via* a molding process. Yuan and his co-authors prepared a light-actuated pH-responsive composite hydrogel by molding-based methods of fabrication. Triggering and terminating the water-oxidation reaction leads to a programmatic expansion and contraction of the active layer, which induces different modes of biomimetic curling motions in the bilayer actuator in light and dark environments.[152] However, a micromolding technique is used to fabricate microstrips combining a micromold built up by conventional photolithography-based techniques to yield complicated microchannel structures with arbitrary geometries.[153] For example, Oh *et al.*[154] explored a basic self-bendable "Janus microstrip" system based on a pH-sensitive hydrogel microstrip as the "active layer" and a nonreactive thin film as the "passive layer" under the influence of biaxial stresses.

3.3.2 Lithographic methodologies. With the invention of the point contact transistor and the requirement of smaller and cheaper semiconductor devices, several important technological trends, such as lithography, were rapidly established. Furthermore, a lithographic process using a spin-coated polymeric film on a substrate was employed. During the lithographic process, a desired pattern is first generated within a resist layer. After that, the desired pattern is transferred to the underlying substrate *via* etching, ion implantation or diffusion. Depending on the different types of transfer, several kinds of lithography were achieved, such as UV-Vis lithography, X-ray electron and electron beam lithography. Using lithography in association with self-folding actuators, it is possible to engineer hollow encapsulants with precise and reproducible shape and size. By means of spin-coating and dip-coating, highly uniform polymer films can be formed and nanometer film thickness can be achieved. Hence, precisely patterned, hollow complex shapes with overall sizes ranging from 100 nm to 1 cm can be fabricated with a variety of materials, including metals, ceramics, and polymers.[155] Benefiting from the advanced strategy, lithographic methodologies are widely utilized in the fabrication of hydrogel actuators to manufacture thin hydrogel scaffolds and obtain accurate and precise patterns.

Photolithography is composed of operating a mask with the desired geometric patterns and subsequently transferring the

pattern to light-sensitive materials *via* irradiation with ultraviolet light. Based on this strategy, Kumar *et al.*[156] formed self-rolled polymer bilayer microtubes. A polymer bilayer was first created by consecutive deposition of poly(4-vinylpyridine) (P4VP) from chloroform and poly(4-bromostyrene) (BrPS) dissolved in toluene on a silicon wafer, by dip-coating. Then, photolithography was used for patterning the bilayer with a UV lamp having a 2.5 W output at 254 nm to irradiate the P4VP/BrPS bilayer. Here, TEM copper grids were used as a photomask, and UV irradiation caused crosslinking between P4VP and BrPS in the irradiated area. The geometric patterns were developed by washing the uncured polymer with a solvent. Such methods rely primarily on photopolymerization of liquid precursors, hence they are only appropriate for photocrosslinkable hydrogels. Moreover, for the fabrication of micro-dimensions in such processes (*e.g.*, microfluidics, microchannels), complicated and expensive external devices or platforms in a special cleaning room are required (Fig. 11).

Soft lithography, which employs elastomeric stamps fabricated from patterned silicon wafers to print or mold materials, is commonly used in 3D microstructure fabrication.[157] Besides that, the combination of two lithographic methodologies has been used in fabricating nano- and microstructures to control the geometric size and shape of hydrogels. Thus, for example, a method for preparing PEG or PEGDA hydrogel structures using electron beam lithography and ultraviolet optical lithography as nano- and micro-fabrication techniques has been reported.[158] Here, E-beam lithography operates with a very high resolution for small structures with a low rate of production. Conversely, UV lithography yields a much higher rate of production, but the resolution is lower. However, with these above-mentioned methods it is difficult to prepare large-sized masks or templates with elaborate patterns, especially those with well-defined, programmable variation in crosslinking densities.[62]

3.3.3 3D printing technologies. 3D printing as a burgeoning digital fabrication technique benefiting from a controllably precise computer-aided design (CAD) model enables the development of intricate actuators with less fabrication and post-processing time, and the least amount of waste material and thus lower cost.[159–161] Hence, 3D printing has been utilized to develop soft actuators in soft robotics, such as origami, self-assembly actuators, self-healing, and biomedical soft actuators.[162] Because 3D soft actuators can be fabricated by 3D printers with custom geometries, functionalities and controlled properties, the combination between the programmable 3D printing and stimuli-responsive materials to produce complex and controllable smart 3D hydrogel actuators promises to yield rewarding results. Zolfagharian *et al.*[161] employed the 3D printing technology to present for the first time a 3D printed soft hydrogel actuator with contactless electrodes (Fig. 12-I). This 3D printed hydrogel soft actuator used the natural polyelectrolyte chitosan as a base material due to its good rheological properties during printing and its mechanical properties both in the dry and in the hydrated state. A special feature of this hydrogel is that the actuation of the hydrogel can be triggered by the pH and ionic strength of the medium, with the voltage on the electrodes being based on the electro-osmotic swelling response. Furthermore, the geometrical properties of the structure and its high porosity are also attributable to the actuation motion. Bakarich *et al.*[163] designed a new ink for 3D printing of hydrogels and fabricated a smart valve that controls the flow of water (Fig. 12-II). Such a hydrogel containing PNIPAM showed revisable changes in length when heated and cooled between 20 °C and 60 °C. Unfortunately, 3D printing is limited in printable hydrogel selection due to the specific viscosity requirement of suitable inks.

3.3.4 Ion inkjet printing. As a well-developed printing technique, computer-assisted inkjet printing is widely used in

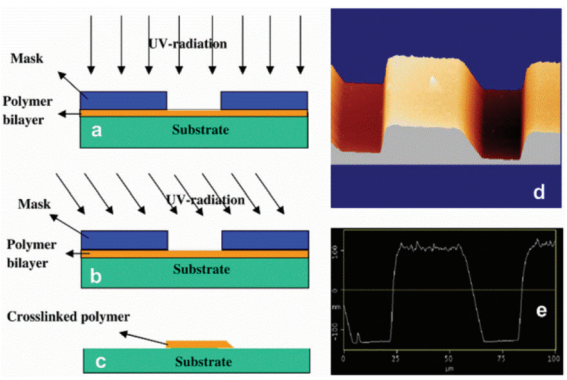

Fig. 11 The photolithography process and schematic way of formation of asymmetric pattern. Reprinted & reproduced with permission from ref. 156. Copyright (2008), Elsevier.

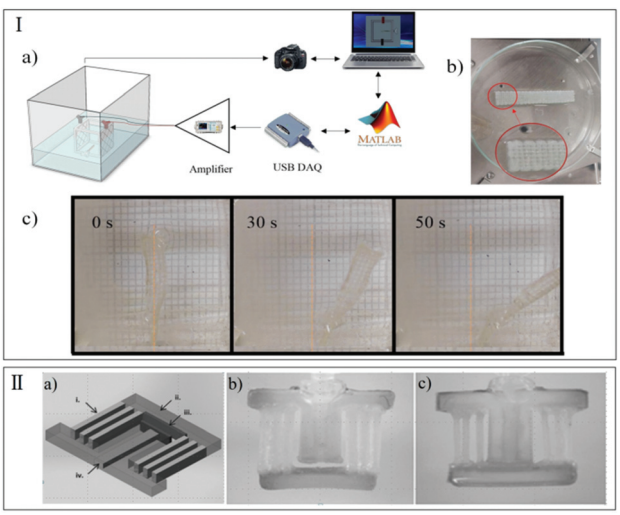

Fig. 12 3D printing technologies: (I) 3D printed hydrogel beam actuator (reprinted & reproduced with permission from ref. 161. Copyright 2017, Elsevier B.V.); (II) computer-aided design model of hydrogel valve and its swollen and shrunken behaviors in water at 20 °C and 60 °C, respectively (reprinted with permission from ref. 163. Copyright 2015, Wiley-VCH Verlag GmbH & Co. KGaA).

everyday work and in our daily life for printing texts and photos. With the development of computer-aided designs and printing equipments, traditional inkjet printing has been applied in areas of science as a new technique, such as patterning materials for microfluidic analytical devices and bioprinted tissues. Peng *et al.*[62] described such a facile and versatile computer-assisted ion inkjet printing technique for hydrogels, which enables the direct printing of many complicated patterns on a large-sized hydrogel in a batch production, especially those with well defined, programmable variations in crosslinking densities, on one or both surfaces of a large-sized hydrogel (Fig. 13). Utilizing a commercial inkjet printer and an aqueous ferric solution, the ferric solution was used as the ink and was printed onto the surface of a pre-synthesized hydrogel containing poly(sodium acrylate). Thus, strong ionic interactions took place between Fe^{3+} cations and the anionic carboxyl groups of poly(sodium acrylate), and then the introduction of metal ions altered the crosslinking densities of the printed area, which led to the different swelling and deswelling behaviors between the unprinted and the printed regions. As a result of that, the shape deformations of the hydrogels were induced. A special advantage of this method is that the deformation rates and degrees of the hydrogel can be adjusted by changing the crosslinking densities *via* controlling the printing time. Benefiting from the convenience and diversity in the designing and printing of this technique, more complicated 3D patterns can be obtained.

3.3.5 Ionoprinting. Ionoprinting is another method that can be used for the patterning of hydrogel containing polyelectrolytes.[164] In contrast to ion inkjet printing, ionoprinting enables not only a modification of the hydrogel at the surface but also induces changes in the bulk, resulting in deep ionoprinting patterns. The principle of the ionoprinting method is based on introducing metal cations into hydrogels *via* the assistance of electrical signals. Thus, the ion printed regions with metal cations stimulate ionic crosslinking of the metal cations and the polyelectrolytes. It is this ionic crosslinking which leads to a reduction in hydrogel water content and in volume. As a result, ionoprinting introduces inhomogeneity into a hydrogel, and thus, a corresponding inhomogeneous shape change is achieved. Moreover, the structure deformation changes with ionoprinting current and imprinted depth, which means more complex deformations can be achieved. Palleau *et al.*[60] first demonstrated the electrical and directional embedding of ions within hydrated gel networks, and locally crosslinking and mechanically stiffening the hydrogel *via* introducing the ionoprinting technique with the capability of topographically structuring and actuating hydrated gels in two and three dimensions by locally patterning ions, assisted by electric fields (Fig. 14-I). In their study, an oxidative bias was applied to a patterned copper anode, which delivered ions to sodium polyacrylate hydrogels as a result of the current passing through the gel. Then, the Cu^{2+} ions generated at the anode/hydrated gel interface associated with the anionic carboxylic groups of the polymer forming robust localized ionic crosslinks in the gel network. Because of the decreasing hydration state in the polymer backbone, the imprinted areas of the network release water, leading to a directional shrinking of the gel. Additionally, the gel composition, the imprinting time and the applied voltage amplitude can be used to change the depth of the ionoprinting patterns. The subsequent investigation yielded that the shape changes were made possible by incorporating two active gel layers and combining them with the ionic crosslinking technique of ionoprinting. Morales *et al.*[63] investigated multi-responsive and double-folding bilayer hydrogel actuators by combining thermoresponsive poly(*N*-isopropyl acrylamide) (PNIPAM) with superabsorbent poly(sodium acrylate) (pNaAc) gels (Fig. 14-II). These actuators can transform into unique 3D shapes with a rapid response time. In their study, external ionoprints reliably and repeatedly invert the gel bilayer bending axis between water and EtOH. Moreover, the directional bending response can be tuned by modulating the solvent quality and the temperature of the external solution. Recently, Baker[165] utilized ionoprinting and iron coordination chemistry to fabricate a thermally induced reversible and reprogrammable actuation of tough hydrogels (Fig. 14-III). In this study, a dual pH-temperature responsive hydrogel derived from *N*-isopropyl acrylamide (NIPAM) and 2-(methacryloyloxy)ethyl phosphate (MOEP) was programmed to undergo a reversible shape change and actuation through ionoprinting of hinges.

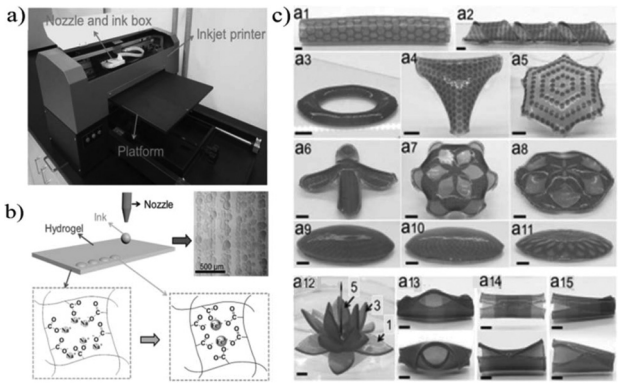

Fig. 13 Ion inkjet printing technique: (a) photograph of flatbed inkjet printer, (b) schematic of the inkjet printing process and image of printed dots on the hydrogel surface as well as cross-linking between ferric ions and anionic carboxyl groups of PNaAAc; (c) complex 3D shapes deformed from 2D patterned hydrogel sheets, including 3D shapes deformed from hydrogels with patterns printed on only one surface (reprinted with permission from ref. 146. Copyright 2017, Wiley-VCH Verlag GmbH & Co. KGaA).

3.3.6 Hydrogel actuators as responsive instruments for cheap open technology (HARICOT). The preparation of hydrogel actuators is in most cases cumbersome and expensive, as aforementioned. Here we will show how to prepare versatile hydrogel actuators in a simple and cheap newly developed process. Velders *et al.* fabricated a hydrogel/textile mixed actuator based on sodium polyacrylate hydrogel (NaPA) beads, which is a well-known super-adsorbing polymer used as a water absorber in applications ranging from drying agents to

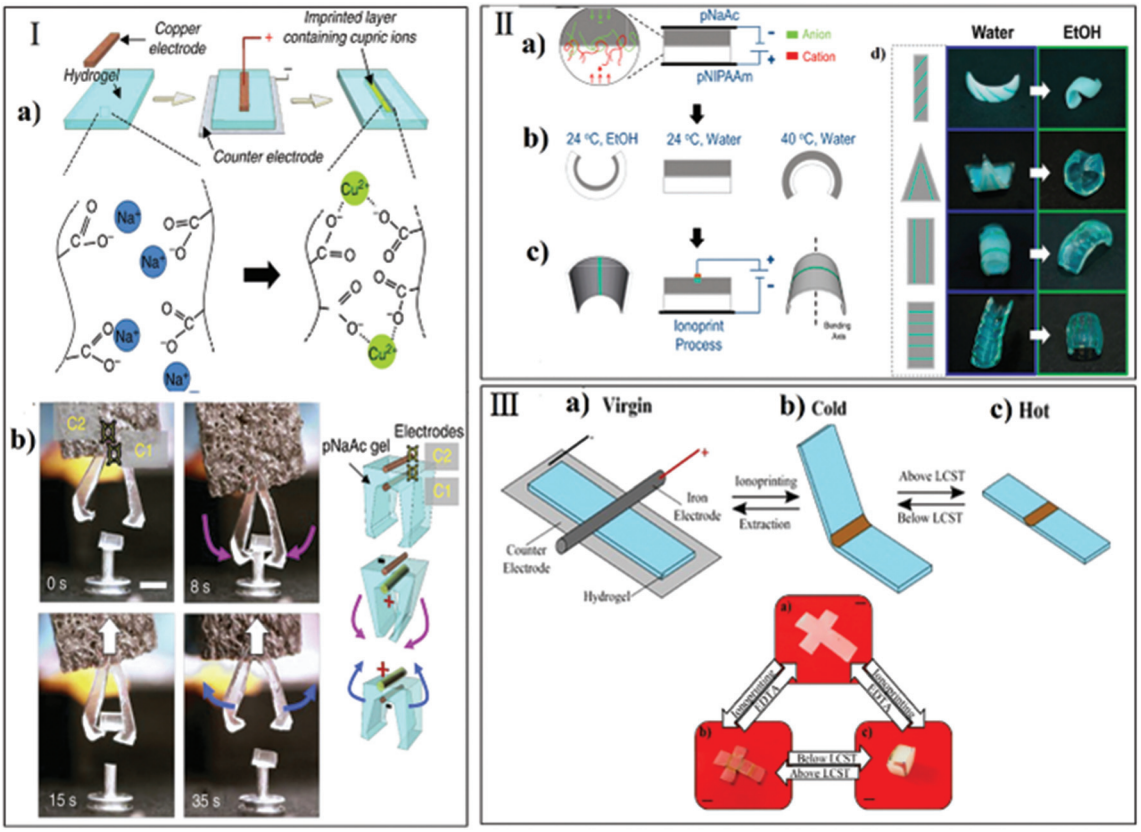

Fig. 14 The ionoprinting technique. (I) Patterned Cu anode with anionic hydrogels to fabricate an ionoprinted hydrogel cylinder. Reprinted with permission from ref. 60. Copyright 2013, Nature Communications; (II) a hydrogel bilayer bending axis orthogonal to the ionoprint direction and bending axis between water and EtOH. Reprinted with permission from ref. 63. Copyright 2016, MDPI; (III) an ionoprinted hydrogel folded and unfolded, oscillating between below LCST and above LCST, respectively (reprinted with permission from ref. 165. Copyright 2017, Elsevier B.V.).

diapers (Fig. 15).[166] The cheap and commercial NaPA hydrogel beads are attached on a strain-directing layer one by one *via* colophony based glue to fabricate HARICOT actuators. A cotton textile, polypropylene plastic, parafilm, and aluminum foil can be used successfully as the strain-directing layer. When the actuators are immersed in water, the NaPA absorbs water and swells, which bends the strain-directing layer and the actuator closes in a loop. In addition, the HARICOT can achieve a muscle movement by gluing NaPA beads on a cotton fabric strip at an interval of 1 cm first and then gluing a second strip to the first strip between the gaps. Because of the expansion of the beads, the cotton textile contracts and the actuator achieves a muscle movement. The methodology has the advantage of being easy and low-cost to achieve *via* facile materials. Importantly, other stimuli-responsive hydrogel-based actuators can be easily fabricated using this simple and cheap process.

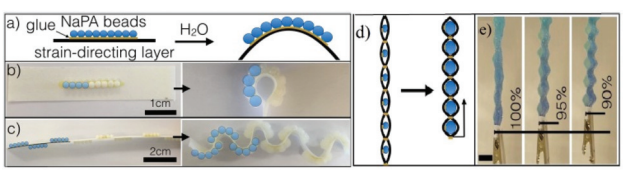

Fig. 15 Schematic of the HARICOT. (a) Illustrated schematic. (b and c) Actuators with NaPA beads attached to the surface and the opposite parts of the paper layer before and after the swelling. (d) Schematics of the working principle of the muscle-like actuator; (e) example of a muscle, before and after the swelling (reprinted with permission from ref. 169. Copyright 2017, Elsevier Ltd).

3.4 Application

Stimuli-responsive hydrogels have been used in designing micromanipulators, sensors, and optical devices with tunable focal length, in control of liquid flow in microfluidic devices, *etc*. For example, Kim *et al.*[167] developed a hydrogel actuator that walks in one direction by using alternating cycles of heating and cooling (Fig. 16-I), unlike the unidirectionally proceeding soft actuator with an external physical bias, such as ratchet-patterned bases or directional stimuli. Here a hydrogel actuator with an L-shaped symmetrical bipedal walker was designed to adopt a layered structure with cofacially oriented unilamellar electrolyte titanate(IV) nanosheets, with the tilt direction of the titanate(IV) nanosheets identifying the forefoot and the backfoot. Upon heating from 25 °C to 45 °C, the backfoot of this object elongates and kicks the base, causing the

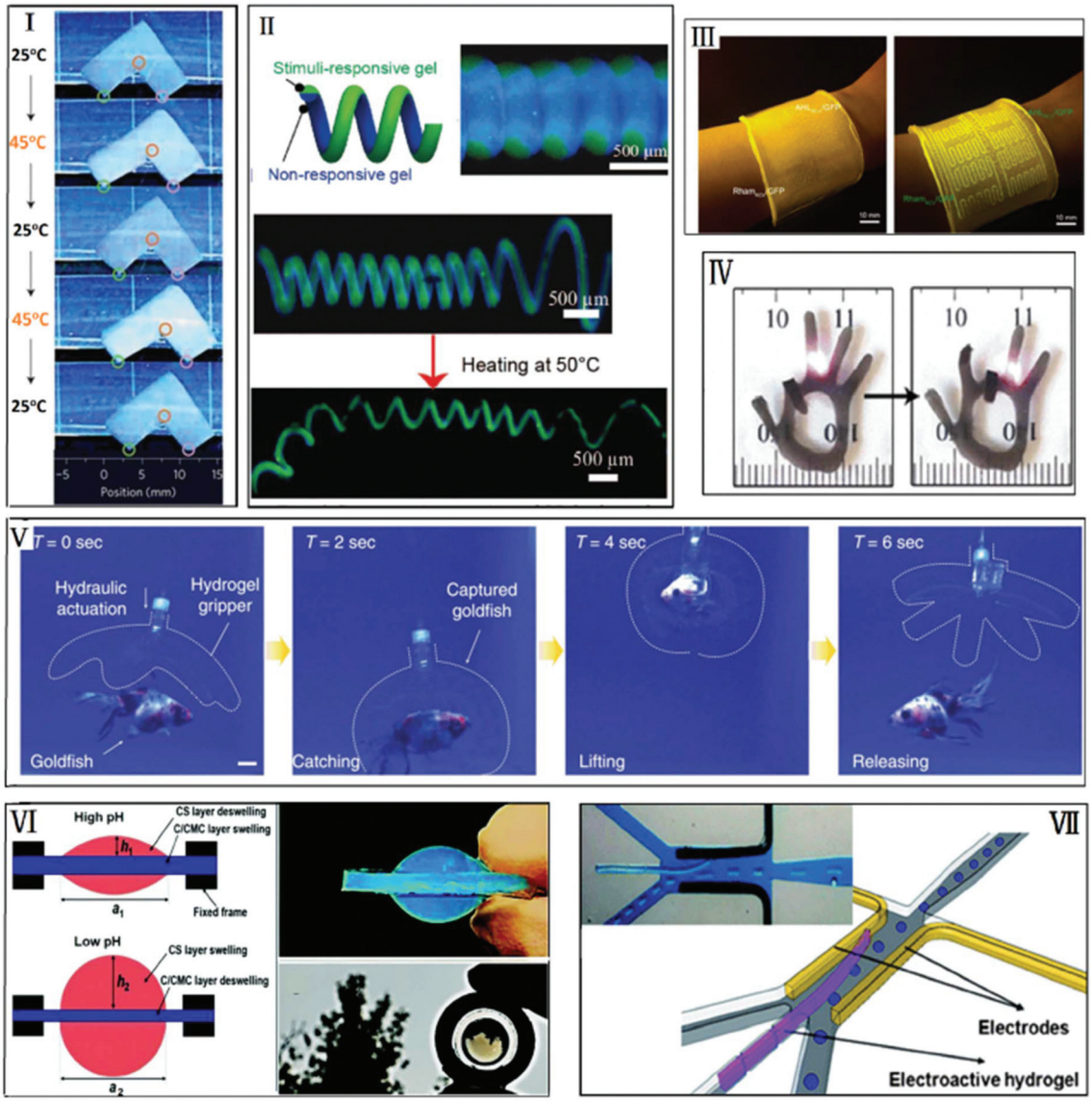

Fig. 16 Examples of hydrogel actuators used in several applications: (I) an L-shaped hydrogel walker fabricated from a PNIPA hydrogel with oriented unilamellar electrolyte titanate nanosheets which can act as a unidirectionally proceeding actuator. Reprinted from ref. 167 with permission, Copyright 2015, Nature publication; (II) a microspring based on an alginate and poly(*N*-isopropylacrylamide-*co*-acrylic acid) hydrogel. Reprinted with permission from ref. 168. Copyright 2017, Nature publication; (III) a hydrogel–elastomer hybrid with four isolated chambers hosting different bacterial strains to sense their cognate inducers visually. Reprinted with permission from ref. 169. Copyright 2017, United States National Academy of Sciences; (IV) joint-like flexing motions of a light-controlled nanocomposite hydrogel hand, reprinted with permission from ref. 170. Copyright 2013, American Chemical Society; (V) agile and transparent hydrogel gripper for catching and releasing a live goldfish. Reprinted with permission from ref. 121. Copyright 2017, Nature publication; (VI) a bioinspired lens based on a bilayer hydrogel. Reprinted with permission from ref. 151, Copyright 2017, The Royal Society of Chemistry; (VII) a microfluidic channel based on an electroactive hydrogel to sort and guide droplets. Reprinted with permission from ref. 10, Copyright 2010, Royal Society of Chemistry.

object to walk forward *via* an internal mechanism for anisotropic energy conversion, meanwhile, its center of mass shifts from its bend point towards the front side. When cooling, the object shortens its elongated backfoot and is drawn backward. However, interestingly, the center of mass shift can potentially suppress this backward motion. Inspired by living bio-actuators such as a stalk in *Vorticella*, Yoshida *et al.*[168] applied a spring-shaped structure to fabricate a hydrogel actuator to magnify its deformation degree (Fig. 16-II). The large compression/expansion motion of such a micro-spring can be controlled by changing the pattern of a stimuli-responsive hydrogel component. These stimuli-responsive hydrogel microsprings have immense potential to be applied in various micro-engineering products, including soft actuators, chemical sensors, and medical applications. A living wearable patch that detects chemicals on the skin was fabricated by a bilayer

hybrid structure of the hydrogel and elastomer, which can conformally attach to the human skin.[169] Such a hydrogel–elastomer hybrid has four isolated chambers hosting different bacterial strains that can sense their cognate inducers (*i.e.*, *N*-acyl homoserine lactone, isopropyl β-D-1-thiogalactopyranoside, and rhamnose) visually. In Fig. 16-III, the hand with an inducer showed a fluorescent glow. Hence, these kinds of functional living devices can be potentially utilized in chemical detection, scientific research and translational medicine in the future. Using thermo-responsive hydrogel composites with graphene oxide nanosheets, Wang *et al.*[170] created light-controlled nanocomposite hydrogel actuators that exhibit diverse mechanical motions by controlling their shape and surface patterns. By modulating laser positioning, timing, and movement, the patterned hand-shaped matrix created joint-like flexing motions upon sequential irradiation (Fig. 16-IV). Surprisingly, Yuk *et al.*[121] developed an agile and camouflaged hydrogel-based actuator to imitate the capabilities of leptocephali, which are high-speed, high-force, and being optically and sonically camouflaged in water. What is even more interesting is that these agile and transparent hydrogel actuators can perform extraordinary functions, like robots, including a hydrogel robotic fish that can achieve forward fishlike locomotion (swimming), an actuator that can kick off a ball, and a camouflaged hydrogel gripper that can even catch and release a live goldfish (Fig. 16-V). Inspired by the focusing strategy of a human lens, a bioinspired flying saucer-like smart lens with a tunable-focus adjusted by the swelling/deswelling behaviors of a bilayer hydrogel was fabricated (Fig. 16-VI).[151] Mimicking the human lens with an asymmetric biconvex structure connected to a ciliary muscle, such a bioinspired lens device consisted of two "caps". These caps are shrunk under a high pH value, leading to flattening, similar to the human lens which relaxes when the person it belongs to has a rest and makes the crystalline lens appear 'flattened', whereas, the caps are swollen under a low pH value, leading to the rounded shape. These optical lenses with a tunable focus *via* adjusting the flattened- and rounded-state are required for potential application in many fields, such as consumer electronics, medical diagnostics, and optical communications. A microfluidic system like a micro-valve to control the liquid flow is one of the potential applications of a micro-hydrogel actuator. Another example is to use the microfluidic channel to sort and guide droplets generated by using a cascading droplet generation channel to demonstrate the visual operation of the electroactive hydrogel actuator (Fig. 16-VII).[10]

4 Summary and outlook

Nature inspired us with a variety of ideas to develop novel structures and to mimic natural properties, such as pinecone seeds that fall down because the hydrated pinecone has dried up. Based on the phenomena of reversible "on–off" switches, scientists learned the mechanism and principles of various motions in nature and further transferred the knowledge from nature to synthetic materials for designing hydrogel-based smart actuators. Then, attempts to utilize these artificial hydrogel actuators in different possible applications, such as bioapplications, have been developed. In this review, we presented two kinds of remarkable "smart" hydrogels inspired by nature, *i.e.*, shape memory hydrogels (SMHs) and stimuli-responsive hydrogels (actuators) (SRHs). We also presented different types of SMHs and discussed the effect individual factors have on shape memory. Additionally, the stimuli-responsive hydrogels used to fabricate actuators have been illustrated and exemplified depending on the types of environmental stimuli, such as physical, chemical and biochemical stimuli. Furthermore, several strategies for manufacturing smart hydrogels with inhomogeneous structures and fabrication technologies adopted in hydrogel-based actuators have been discussed and summarized. Yet there is still a long way to go in producing complex deformations from 2D to 3D, just like general and collaborative multi-step actuation in natural life, partly because chemical structures sensitive to multi-stimuli should be combined in a hydrogel matrix to achieve multi-step actuation imitating natural life. Furthermore, intrinsic interest on new and different chemical approaches and their external stimulation should be investigated more. In addition, the sequence control and the time-consuming process of hydrogels with a complex deformation are still challenging to achieve with the current fabrication techniques. Hence, trends of "smart" hydrogels are to develop the formation of multi-stimulative hydrogels with complex but programmed self-folding, twisting and bending behaviors by designing inhomogeneous hydrogels through the creation of improved fabrication technologies.

Conflicts of interest

There are no conflicts to declare.

Acknowledgements

J. S. gratefully acknowledges the China Scholarship Council (CSC grant: 201406240131) for partial financial support of this work.

References

1 R. Fernandes and D. H. Gracias, *Adv. Drug Delivery Rev.*, 2012, **64**, 1579–1589.
2 M. A. Ward and T. K. Georgiou, *Polymer*, 2011, **3**, 1215–1242.
3 T. Kumar Giri, D. Thakur, Ajazuddin, H. Badwaik and D. Krishna Tripathi, *Curr. Drug Delivery*, 2012, **9**, 539–555.
4 I. Strehin, Z. Nahas, K. Arora, T. Nguyen and J. Elisseeff, *Biomaterials*, 2010, **31**, 2788–2797.
5 P. N. Charron, S. L. Fenn, A. Poniz and R. A. Oldinski, *J. Mech. Behav. Biomed. Mater.*, 2016, **59**, 314–321.

6 N. T. Phuong, V. A. Ho, D. H. Nguyen, N. C. Khoa, T. N. Quyen, Y. Lee and K. D. Park, *J. Bioact. Compat. Polym.*, 2015, **30**, 412–423.
7 R. Jin and P. J. Dijkstra, *Biomed. Appl. Hydrogels Handb.*, 2010, **101**, 203–225.
8 I. Vasiev, A. I. M. Greer, A. Z. Khokhar, J. Stormonth-Darling, K. E. Tanner and N. Gadegaard, *Microelectron. Eng.*, 2013, **108**, 76–81.
9 S. Zakharchenko, N. Puretskiy, G. Stoychev, M. Stamm and L. Ionov, *Soft Matter*, 2010, **6**, 2633–2636.
10 G. H. Kwon, Y. Y. Choi, J. Y. Park, D. H. Woo, K. B. Lee, J. H. Kim and S. H. Lee, *Lab Chip*, 2010, **10**, 1604–1610.
11 S. Maeda, Y. Hara, R. Yoshida and S. Hashimoto, *Int. J. Mol. Sci.*, 2010, **11**, 52–66.
12 C. Ma, W. Lu, X. Yang, J. He, X. Le, L. Wang, J. Zhang, M. J. Serpe, Y. Huang and T. Chen, *Adv. Funct. Mater.*, 2018, **28**, 1704568.
13 A. Mateescu, Y. Wang, J. Dostalek and U. Jonas, *Membranes*, 2012, **2**, 40–49.
14 M. Hasnat Kabir, T. Hazama, Y. Watanabe, J. Gong, K. Murase, T. Sunada and H. Furukawa, *J. Taiwan Inst. Chem. Eng.*, 2014, **45**, 3134–3138.
15 H. Ko and A. Javey, *Acc. Chem. Res.*, 2017, **50**, 691–702.
16 M. P. M. Dicker, A. B. Baker, R. J. Iredale, S. Naficy, I. P. Bond, C. F. J. Faul, J. M. Rossiter, G. M. Spinks and P. M. Weaver, *Sci. Rep.*, 2017, **7**, 9197.
17 T. Shen, M. G. Font, S. Jung, M. L. Gabriel, M. P. Stoykovich and F. J. Vernerey, *Sci. Rep.*, 2017, **7**, 1–10.
18 B. Q. Y. Chan, Z. W. K. Low, S. J. W. Heng, S. Y. Chan, C. Owh and X. J. Loh, *ACS Appl. Mater. Interfaces*, 2016, **8**, 10070–10087.
19 W. Lu, X. Le, J. Zhang, Y. Huang and T. Chen, *Chem. Soc. Rev.*, 2017, **46**, 1284–1294.
20 C. Löwenberg, M. Balk, C. Wischke, M. Behl and A. Lendlein, *Acc. Chem. Res.*, 2017, **50**, 723–732.
21 W. Wang, Y. Zhang and W. Liu, *Prog. Polym. Sci.*, 2017, **71**, 1–25.
22 R. Luo, J. Wu, N. D. Dinh and C. H. Chen, *Adv. Funct. Mater.*, 2015, **25**, 7272–7279.
23 Y. Zhang, J. Liao, T. Wang, W. Sun and Z. Tong, *Adv. Funct. Mater.*, 2018, **28**, 1–9.
24 J. You, S. Xie, J. Cao, H. Ge, M. Xu, L. Zhang and J. Zhou, *Macromolecules*, 2016, **49**, 1049–1059.
25 K. Peng, H. Yu, H. Yang, X. Hao, A. Yasin and X. Zhang, *Soft Matter*, 2017, **13**, 2135–2140.
26 T. Tanaka, E. Sato, Y. Hirokawa, S. Hirotsu and J. Peetermans, *Phys. Rev. Lett.*, 1985, **55**, 2455–2458.
27 S. Ma, B. Yu, X. Pei and F. Zhou, *Polymer*, 2016, **98**, 516–535.
28 C. Yao, Z. Liu, C. Yang, W. Wang, X. J. Ju, R. Xie and L. Y. Chu, *ACS Appl. Mater. Interfaces*, 2016, **8**, 21721–21730.
29 Z. J. Wang, C. N. Zhu, W. Hong, Z. Liang Wu and Q. Zheng, *Sci. Adv.*, 2017, **3**, e1700348.
30 H. Wang, Q. Shi, T. Yue, M. Nakajima, M. Takeuchi, Q. Huang and T. Fukuda, *Int. J. Adv. Robot. Syst.*, 2014, **11**, 115–127.
31 A. Richter, G. Paschew, S. Klatt, J. Lienig, K. F. Arndt and H. J. P. Adler, *Sensors*, 2008, **8**, 561–581.
32 S. Zhao, Y. Chen, B. P. Partlow, A. S. Golding, P. Tseng, J. Coburn, M. B. Applegate, J. E. Moreau, F. G. Omenetto and D. L. Kaplan, *Biomaterials*, 2016, **93**, 60–70.
33 T. Matsuda, T. Nakajima, Y. Fukuda, W. Hong, T. Sakai, T. Kurokawa, U. Il Chung and J. P. Gong, *Macromolecules*, 2016, **49**, 1865–1872.
34 Y. Zhao, T. Nakajima, J. J. Yang, T. Kurokawa, J. Liu, J. Lu, S. Mizumoto, K. Sugahara, N. Kitamura, K. Yasuda, A. U. D. Daniels and J. P. Gong, *Adv. Mater.*, 2014, **26**, 436–442.
35 T. C. Suekama, J. Hu, T. Kurokawa, J. P. Gong and S. H. Gehrke, *ACS Macro Lett.*, 2013, **2**, 137–140.
36 Y. Bu, H. Shen, F. Yang, Y. Yang, X. Wang and D. Wu, *ACS Appl. Mater. Interfaces*, 2017, **9**, 2205–2212.
37 T. Nakajima, H. Sato, Y. Zhao, S. Kawahara, T. Kurokawa, K. Sugahara and J. P. Gong, *Adv. Funct. Mater.*, 2012, **22**, 4426–4432.
38 J. Hao and R. A. Weiss, *ACS Macro Lett.*, 2013, **2**, 86–89.
39 J. Huang, L. Zhao, T. Wang, W. Sun and Z. Tong, *ACS Appl. Mater. Interfaces*, 2016, **8**, 12384–12392.
40 X. X. Le, Y. C. Zhang, W. Lu, L. Wang, J. Zheng, I. Ali, J. W. Zhang, Y. J. Huang, M. J. Serpe, X. T. Yang, X. D. Fan and T. Chen, *Macromol. Rapid Commun.*, 2018, **39**, 1–6.
41 Y. Han, T. Bai, Y. Liu, X. Zhai and W. Liu, *Macromol. Rapid Commun.*, 2012, **33**, 225–231.
42 U. Nöchel, M. Behl, M. Balk and A. Lendlein, *ACS Appl. Mater. Interfaces*, 2016, **8**, 28068–28076.
43 X. Le, W. Lu, J. Zheng, D. Tong, N. Zhao, C. Ma, H. Xiao, J. Zhang, Y. Huang and T. Chen, *Chem. Sci.*, 2016, **7**, 6715–6720.
44 H. Xiao, W. Lu, X. Le, C. Ma, Z. Li, J. Zheng, J. Zhang, Y. Huang and T. Chen, *Chem. Commun.*, 2016, **52**, 13292–13295.
45 X. Le, W. Lu, H. Xiao, L. Wang, C. Ma, J. Zhang, Y. Huang and T. Chen, *ACS Appl. Mater. Interfaces*, 2017, **9**, 9038–9044.
46 Y.-Y. Xiao, X.-L. Gong, Y. Kang, Z.-C. Jiang, S. Zhang and B.-J. Li, *Chem. Commun.*, 2016, **52**, 10609–10612.
47 X.-L. Gong, Y.-Y. Xiao, M. Pan, Y. Kang, B.-J. Li and S. Zhang, *ACS Appl. Mater. Interfaces*, 2016, **8**, 27432–27437.
48 L. Zhao, J. Huang, T. Wang, W. Sun and Z. Tong, *Macromol. Mater. Eng.*, 2017, **302**, 1600359.
49 H. Xiao, C. Ma, X. Le, L. Wang, W. Lu, P. Theato, T. Hu, J. Zhang and T. Chen, *Polymer*, 2017, **9**, 138–148.
50 H. Meng, P. Xiao, J. Gu, X. Wen, J. Xu, C. Zhao, J. Zhang and T. Chen, *Chem. Commun.*, 2014, **50**, 12277–12280.
51 G. Li, H. Zhang, D. Fortin, H. Xia and Y. Zhao, *Langmuir*, 2015, **31**, 11709–11716.
52 Y. Fan, W. Zhou, A. Yasin, H. Li and H. Yang, *Soft Matter*, 2015, **11**, 4218–4225.

53 K. Peng, H. Yu, H. Yang, X. Hao, A. Yasin and X. Zhang, *Soft Matter*, 2017, **13**, 2135–2140.
54 L. Wang, Y. Jian, X. Le, W. Lu, C. Ma, J. Zhang, Y. Huang, C. F. Huang and T. Chen, *Chem. Commun.*, 2018, **54**, 1229–1232.
55 Z. Li, W. Lu, T. Ngai, X. Le, J. Zheng, N. Zhao, Y. Huang, X. Wen, J. Zhang and T. Chen, *Polym. Chem.*, 2016, **7**, 5343–5346.
56 B. Xu, Y. Li, F. Gao, X. Zhai, M. Sun, W. Lu, Z. Cao and W. Liu, *ACS Appl. Mater. Interfaces*, 2015, **7**, 16865–16872.
57 D. H. Gracias, *Curr. Opin. Chem. Eng.*, 2013, **2**, 112–119.
58 J. Kim, J. A. Hanna, M. Byun, C. D. Santangelo and R. C. Hayward, *Science*, 2012, **1201**, 1200–1205.
59 J. Kim, J. a. Hanna, R. C. Hayward and C. D. Santangelo, *Soft Matter*, 2012, **8**, 2375–2381.
60 E. Palleau, D. Morales, M. D. Dickey and O. D. Velev, *Nat. Commun.*, 2013, **4**, 1–7.
61 J. Wang, J. Wang, Z. Chen, S. Fang, Y. Zhu, R. H. Baughman and L. Jiang, *Chem. Mater.*, 2017, **29**, 9793–9801.
62 X. Peng, T. Liu, Q. Zhang, C. Shang, Q. W. Bai and H. Wang, *Adv. Funct. Mater.*, 2017, **27**, 1–8.
63 D. Morales, I. Podolsky, R. W. Mailen, T. Shay, M. D. Dickey and O. D. Velev, *Micromachines*, 2016, **7**, 98.
64 N. Bassik, B. T. Abebe, K. E. Laflin and D. H. Gracias, *Polymer*, 2010, **51**, 6093–6098.
65 L. Zhao, J. Huang, Y. Zhang, T. Wang, W. Sun and Z. Tong, *ACS Appl. Mater. Interfaces*, 2017, **9**, 11866–11873.
66 X. Li, X. Cai, Y. Gao and M. J. Serpe, *J. Mater. Chem. B*, 2017, **5**, 2804–2812.
67 J. Kim, C. Kim, Y. S. Song, S. G. Jeong, T. S. Kim and C. S. Lee, *Chem. Eng. J.*, 2017, **321**, 384–393.
68 I. Tokarev and S. Minko, *Soft Matter*, 2009, **5**, 511–524.
69 M. Dadsetan, Z. Liu, M. Pumberger, C. V. Giraldo, T. Ruesink, L. Lu and M. J. Yaszemski, *Biomaterials*, 2010, **31**, 8051–8062.
70 C. M. Dong and Y. Chen, *J. Controlled Release*, 2011, **152**, e13–e14.
71 H. Li, in *Smart Hydrogel Modelling*, 2009, pp. 173–218.
72 E. M. White, J. Yatvin, J. B. Grubbs, J. A. Bilbrey and J. Locklin, *J. Polym. Sci., Part B: Polym. Phys.*, 2013, **51**, 1084–1099.
73 H. Li, in *Smart Hydrogel Modelling*, 2009, pp. 295–333.
74 T. Morimoto and F. Ashida, *Int. J. Solids Struct.*, 2015, **56**, 20–28.
75 B. Xue, M. Qin, T. Wang, J. Wu, D. Luo, Q. Jiang, Y. Li, Y. Cao and W. Wang, *Adv. Funct. Mater.*, 2016, **26**, 9053–9062.
76 Y. Tan, S. Xu, R. Wu, J. Du, J. Sang and J. Wang, *Appl. Clay Sci.*, 2017, **148**, 77–82.
77 H. Meng, J. Zheng, X. Wen, Z. Cai, J. Zhang and T. Chen, *Macromol. Rapid Commun.*, 2015, **36**, 533–537.
78 K. Zhang, Y. Luo and Z. Li, *Soft Matter*, 2007, **5**, 183–195.
79 J. Kim, N. Singh and L. A. Lyon, *Angew. Chem., Int. Ed.*, 2006, **45**, 1446–1449.
80 J. Hu, G. Zhang and S. Liu, *Chem. Soc. Rev.*, 2012, **41**, 5933–5949.
81 W. C. Liao, S. Lilienthal, J. S. Kahn, M. Riutin, Y. S. Sohn, R. Nechushtai and I. Willner, *Chem. Sci.*, 2017, **8**, 3362–3373.
82 D. Men, L. Hang, H. Zhang, X. Zhang, X. Liu, W. Cai and Y. Li, *ChemNanoMat*, 2018, **4**, 165–169.
83 L. M. Bonanno and U. A. Delouise, *Adv. Funct. Mater.*, 2010, **20**, 573–578.
84 D. Yang, J. Zhao, X. Wang, J. Shi, S. Zhang and Z. Jiang, *Biochem. Eng. J.*, 2017, **117**, 52–61.
85 H. Liu, L. Rong, B. Wang, R. Xie, X. Sui, H. Xu, L. Zhang, Y. Zhong and Z. Mao, *Carbohydr. Polym.*, 2017, **176**, 299–306.
86 J. Park, S. Pramanick, D. Park, J. Yeo, J. Lee, H. Lee and W. J. Kim, *Adv. Mater.*, 2017, **29**, 1702859.
87 J. Du, B. Li, C. Li, Y. Zhang, G. Yu, H. Wang and X. Mu, *Int. J. Biol. Macromol.*, 2016, **88**, 451–456.
88 Q. Zhu, L. Zhang, K. J. Van Vliet, A. Miserez and N. Holten-Andersen, *ACS Appl. Mater. Interfaces*, 2018, **10**, 10409–10418.
89 C. Gong, S. Shi, P. Dong, B. Kan, M. Gou, X. Wang, X. Li, F. Luo, X. Zhao, Y. Wei and Z. Qian, *Int. J. Pharm.*, 2009, **365**, 89–99.
90 M. Prabaharan and J. F. Mano, *Macromol. Biosci.*, 2006, **6**, 991–1008.
91 K. K. Westbrook and H. J. Qi, *J. Intell. Mater. Syst. Struct.*, 2007, **19**, 597–607.
92 C. Yao, Z. Liu, C. Yang, W. Wang, X. J. Ju, R. Xie and L. Y. Chu, *Adv. Funct. Mater.*, 2015, **25**, 2980–2991.
93 M. E. Harmon, M. Tang and C. W. Frank, *Polymer*, 2003, **44**, 4547–4556.
94 H. G. Schild, *Prog. Polym. Sci.*, 1992, **17**, 163–249.
95 S. R. Sershen, G. A. Mensing, M. Ng, N. J. Halas, D. J. Beebe and J. L. West, *Adv. Mater.*, 2005, **17**, 1366–1368.
96 H. Thérien-Aubin, Z. L. Wu, Z. Nie and E. Kumacheva, *J. Am. Chem. Soc.*, 2013, **135**, 4834–4839.
97 W. J. Zheng, N. An, J. H. Yang, J. Zhou and Y. M. Chen, *ACS Appl. Mater. Interfaces*, 2015, **7**, 1758–1764.
98 J. S. Kahn, Y. Hu and I. Willner, *Acc. Chem. Res.*, 2017, **50**, 680–690.
99 L. H. Lima, Y. Morales and T. Cabral, *Int. J. Retina Vitreous*, 2016, **2**, 23.
100 P. Patra, A. P. Rameshbabu, D. Das, S. Dhara, A. B. Panda and S. Pal, *Polym. Chem.*, 2016, **7**, 5426–5435.
101 H. Warren, M. in het Panhuis, G. M. Spinks and D. L. Officer, *J. Polym. Sci., Part B: Polym. Phys.*, 2018, **56**, 46–52.
102 T. Trongsatitkul and B. M. Budhlall, *Polym. Chem.*, 2013, **4**, 1502–1516.
103 T. H. Lee and J. Y. Jho, *Macromol. Res.*, 2018, **26**, 659–664.
104 R. P. Hamlen, C. E. Kent and S. N. Shafer, *Nature*, 1965, **206**, 1149–1150.
105 C. Yang, W. Wang, C. Yao, R. Xie, X. J. Ju, Z. Liu and L. Y. Chu, *Sci. Rep.*, 2015, **5**, 1–10.

106 D. Morales, E. Palleau, M. D. Dickey and O. D. Velev, *Soft Matter*, 2014, **10**, 1337–1348.
107 M. Bassil, J. Davenas and M. EL Tahchi, *Sens. Actuators, B*, 2008, **134**, 496–501.
108 Z. Liu, R. Tang, D. Xu, J. Liu and H. Yu, *Macromol. Rapid Commun.*, 2015, **36**, 1171–1176.
109 Y. H. Chan, M. E. Gallina, X. Zhang, I. C. Wu, Y. Jin, W. Sun and D. T. Chiu, *Anal. Chem.*, 2012, **84**, 9431–9438.
110 Y. S. Nam, I. Yoo, O. Yarimaga, I. S. Park, D.-H. Park, S. Song, J.-M. Kim and C. W. Lee, *Chem. Commun.*, 2014, **50**, 4251–4254.
111 C. H. Zhu, Y. Lu, J. Peng, J. F. Chen and S. H. Yu, *Adv. Funct. Mater.*, 2012, **22**, 4017–4022.
112 E. Lee, H. Lee, S. Il Yoo and J. Yoon, *ACS Appl. Mater. Interfaces*, 2014, **6**, 16949–16955.
113 C. Y. Chou, K. S. Chen, W. L. Lin, Y. C. Ye and S. C. Liao, *Micromachines*, 2017, **8**, 5.
114 E. Lee, D. Kim, H. Kim and J. Yoon, *Sci. Rep.*, 2015, **5**, 1–8.
115 X. Yu, S. Zhou, X. Zheng, T. Guo, Y. Xiao and B. Song, *Nanotechnology*, 2009, **20**, 235702.
116 T. S. Shim, S. H. Kim, C. J. Heo, H. C. Jeon and S. M. Yang, *Angew. Chem., Int. Ed.*, 2012, **51**, 1420–1423.
117 W. Gao, L. Wang, X. Wang and H. Liu, *ACS Appl. Mater. Interfaces*, 2016, **8**, 14182–14189.
118 Z. Tang, C. He, H. Tian, J. Ding, B. S. Hsiao, B. Chu and X. Chen, *Prog. Polym. Sci.*, 2016, **60**, 86–128.
119 M. C. Koetting, J. T. Peters, S. D. Steichen and N. A. Peppas, *Mater. Sci. Eng., R*, 2015, **93**, 1–49.
120 N. S. Nikouei, M. R. Vakili, M. S. Bahniuk, L. Unsworth, A. Akbari, J. Wu and A. Lavasanifar, *Acta Biomater.*, 2015, **12**, 81–92.
121 H. Yuk, S. Lin, C. Ma, M. Takaffoli, N. X. Fang and X. Zhao, *Nat. Commun.*, 2017, **8**, 1–12.
122 G. Chinga-Carrasco and K. Syverud, *J. Biomater. Appl.*, 2014, **29**, 423–432.
123 T. Yokoi, M. Kawashita and C. Ohtsuki, *J. Asian Ceram. Soc.*, 2013, **1**, 155–162.
124 B. Mishra, *Austin J. Biomed. Eng.*, 2017, **4**, 1037.
125 K. U. Jeong, J. H. Jang, D. Y. Kim, C. Nah, J. H. Lee, M. H. Lee, H. J. Sun, C. L. Wang, S. Z. D. Cheng and E. L. Thomas, *J. Mater. Chem.*, 2011, **21**, 6824–6830.
126 C. Legros, M. C. De Pauw-Gillet, K. C. Tam, S. Lecommmandoux and D. Taton, *Polym. Chem.*, 2013, **4**, 4801.
127 S. V. Wegner, F. C. Schenk, S. Witzel, F. Bialas and J. P. Spatz, *Macromolecules*, 2016, **49**, 4229–4235.
128 A. F. Greene, M. K. Danielson, A. O. Delawder, K. P. Liles, X. Li, A. Natraj, A. Wellen and J. C. Barnes, *Chem. Mater.*, 2017, **29**, 9498–9508.
129 Y. Ito, M. Casolaro, K. Kono and Y. Imanishi, *J. Controlled Release*, 1989, **10**, 195–203.
130 D. Shiino, Y. Murata, K. Kataoka, Y. Koyama, M. Yokoyama, T. Okano and Y. Sakurai, *Biomaterials*, 1994, **15**, 121–128.
131 T. Yang, R. Ji, X.-X. Deng, F.-S. Du and Z.-C. Li, *Soft Matter*, 2014, **10**, 2671–2678.
132 J. Cao, S. Liu, Y. Chen, L. Shi and Z. Zhang, *Polym. Chem.*, 2014, **5**, 5029–5036.
133 W. L. A. Brooks, G. Vancoillie, C. P. Kabb, R. Hoogenboom and B. S. Sumerlin, *J. Polym. Sci., Part A: Polym. Chem.*, 2017, **55**, 2309–2317.
134 F. Horkay, S. H. Cho, P. Tathireddy, L. Rieth, F. Solzbacher and J. Magda, *Sens. Actuators, B*, 2011, **160**, 1363–1371.
135 M. D. Phillips and T. D. James, *J. Fluoresc.*, 2004, **14**, 549–559.
136 P. R. Westmark and B. D. Smith, *J. Am. Chem. Soc.*, 1994, **116**, 9343–9344.
137 T. Kawanishi, M. A. Romey, P. C. Zhu, M. Z. Holody and S. Shinkai, *J. Fluoresc.*, 2004, **14**, 499–512.
138 A. Pettignano, S. Grijalvo, M. Häring, R. Eritja, N. Tanchoux, F. Quignard and D. Díaz Díaz, *Chem. Commun.*, 2017, **53**, 3350–3353.
139 Y. Dong, W. Wang, O. Veiseh, E. A. Appel, K. Xue, M. J. Webber, B. C. Tang, X. W. Yang, G. C. Weir, R. Langer and D. G. Anderson, *Langmuir*, 2016, **32**, 8743–8747.
140 D. Roy and B. S. Sumerlin, *ACS Macro Lett.*, 2012, **1**, 529–532.
141 J. C. Athas, C. P. Nguyen, B. C. Zarket, A. Gargava, Z. Nie and S. R. Raghavan, *ACS Appl. Mater. Interfaces*, 2016, **8**, 19066–19074.
142 Z. Sui, W. J. King and W. L. Murphy, *Adv. Mater.*, 2007, **19**, 3377–3380.
143 P. D. Thornton, R. J. Mart and R. V. Ulijn, *Adv. Mater.*, 2007, **19**, 1252–1256.
144 Á. Némethy, K. Solti, L. Kiss, B. Gyarmati, M. A. Deli, E. Csányi and A. Szilágyi, *Eur. Polym. J.*, 2013, **49**, 1268–1286.
145 A. Tamayol, M. Akbari, Y. Zilberman, M. Comotto, E. Lesha, L. Serex, S. Bagherifard, Y. Chen, G. Fu, S. K. Ameri, W. Ruan, E. L. Miller, M. R. Dokmeci, S. Sonkusale and A. Khademhosseini, *Adv. Healthcare Mater.*, 2016, **5**, 711–719.
146 A. Shastri, L. M. McGregor, Y. Liu, V. Harris, H. Nan, M. Mujica, Y. Vasquez, A. Bhattacharya, Y. Ma, M. Aizenberg, O. Kuksenok, A. C. Balazs, J. Aizenberg and X. He, *Nat. Chem.*, 2015, **7**, 447–454.
147 H. Chen and Y. Lo Hsieh, *J. Polym. Sci., Part A: Polym. Chem.*, 2004, **42**, 6331–6339.
148 J. C. Breger, C. Yoon, R. Xiao, H. R. Kwag, M. O. Wang, J. P. Fisher, T. D. Nguyen and D. H. Gracias, *ACS Appl. Mater. Interfaces*, 2015, **7**, 3398–3405.
149 J. Shang and P. Theato, *Soft Matter*, 2018, **14**, 8401–8407.
150 M. Li, Q. Yang, H. Liu, M. Qiu, T. J. Lu and F. Xu, *Small*, 2016, **12**, 4492–4500.
151 J. Duan, X. Liang, K. Zhu, J. Guo and L. Zhang, *Soft Matter*, 2017, **13**, 345–354.
152 P. Yuan, J. M. McCracken, D. E. Gross, P. V. Braun, J. S. Moore and R. G. Nuzzo, *Soft Matter*, 2017, **13**, 7312–7317.
153 Y. Yajima, M. Yamada, E. Yamada, M. Iwase and M. Seki, *Biomicrofluidics*, 2014, **8**, 024115.
154 M. S. Oh, Y. S. Song, C. Kim, J. Kim, J. B. You, T. S. Kim, C. S. Lee and S. G. Im, *ACS Appl. Mater. Interfaces*, 2016, **8**, 8782–8788.

155 C. L. Randall, E. Gultepe and D. H. Gracias, *Trends Biotechnol.*, 2012, **30**, 138–146.
156 K. Kumar, V. Luchnikov, B. Nandan, V. Senkovskyy and M. Stamm, *Eur. Polym. J.*, 2008, **44**, 4115–4121.
157 J. Pan, S. Yung Chan, J. E. A. Common, S. Amini, A. Miserez, E. Birgitte Lane and L. Kang, *J. Biomed. Mater. Res., Part A*, 2013, **101**, 3159–3169.
158 M. Bae, R. A. Gemeinhart, R. Divan, K. J. Suthar and D. C. Mancini, *J. Vac. Sci. Technol., B: Nanotechnol. Microelectron.: Mater., Process., Meas., Phenom.*, 2010, **28**, C6P24–C6P29.
159 A. Zolfagharian, A. Z. Kouzani, S. Y. Khoo, A. A. A. Moghadam, I. Gibson and A. Kaynak, *Sens. Actuators, A*, 2016, **250**, 258–272.
160 A. Zolfagharian, A. Z. Kouzani, B. Nasri-Nasrabadi, S. Adams, S. Yang Khoo, M. Norton, I. Gibson and A. Kaynak, *KnE Eng.*, 2017, **2**, 15–22.
161 A. Zolfagharian, A. Z. Kouzani, S. Y. Khoo, B. Nasri-Nasrabadi and A. Kaynak, *Sens. Actuators, A*, 2017, **265**, 94–101.
162 X. Zhai, Y. Ma, C. Hou, F. Gao, Y. Zhang, C. Ruan, H. Pan, W. W. Lu and W. Liu, *ACS Biomater. Sci. Eng.*, 2017, **3**, 1109–1118.
163 S. E. Bakarich, R. Gorkin, M. In Het Panhuis and G. M. Spinks, *Macromol. Rapid Commun.*, 2015, **36**, 1211–1217.
164 B. P. Lee and S. Konst, *Adv. Mater.*, 2014, **26**, 3415–3419.
165 A. B. Baker, D. F. Wass and R. S. Trask, *Sens. Actuators, B*, 2018, **254**, 519–525.
166 A. H. Velders, J. A. Dijksman and V. Saggiomo, *Appl. Mater. Today*, 2017, **9**, 271–275.
167 Y. S. Kim, M. Liu, Y. Ishida, Y. Ebina, M. Osada, T. Sasaki, T. Hikima, M. Takata and T. Aida, *Nat. Mater.*, 2015, **14**, 1–6.
168 K. Yoshida, S. Nakajima, R. Kawano and H. Onoe, *Sens. Actuators, B*, 2018, **272**, 361–368.
169 X. Liu, T.-C. Tang, E. Tham, H. Yuk, S. Lin, T. K. Lu and X. Zhao, *Proc. Natl. Acad. Sci. U. S. A.*, 2017, **114**, 2200–2205.
170 E. Wang, M. S. Desai and S. Lee, *Nano Lett.*, 2013, **13**, 2826–2830.